



Delft Cluster performs fundamental research for sustainable delta development.

GeoDelft / IHE / TNO /
TU Delft / WL | Delft Hydraulics

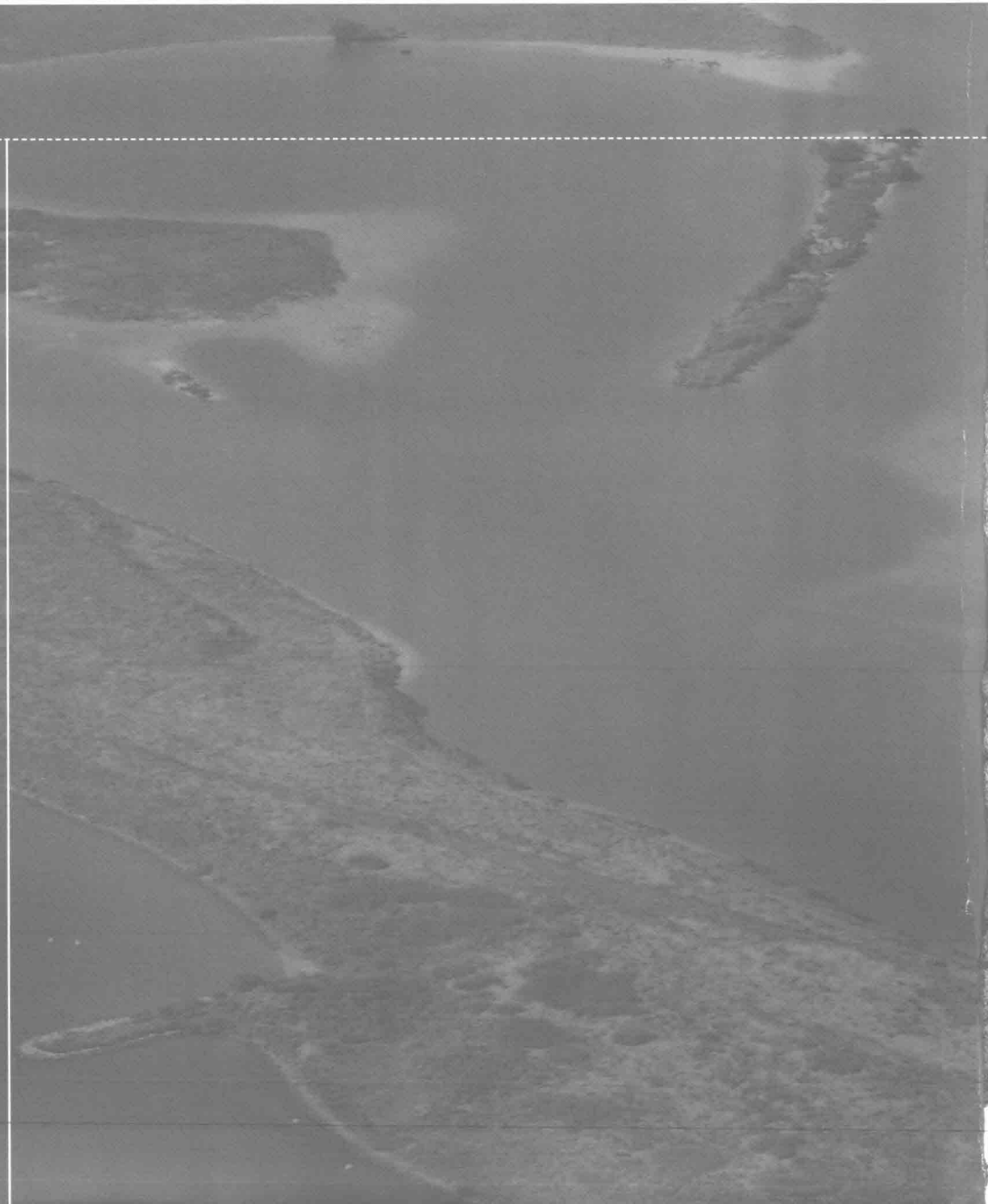
Stability of near-bed structures and bed protections

Analysis of physical model tests with waves and currents

Authors: M.R.A. van Gent
I. Wallast
Date: December 2001
Project identification: DC030204/H3804



PO Box 69 / 2600 AB Delft / The Netherlands
phone +31(0)15-26 93 793 / fax +31(0)15-26 93 799 /
info@delftcluster.nl / www.delftcluster.nl





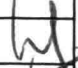


FRAMEWORK: Delft Cluster, Theme 3 'Coast and River', Project 'Behaviour of granular material'

TITLE: Stability of near-bed structures and bed protections
Analysis of physical model tests with waves and currents

ABSTRACT: In river and coastal engineering bed protections and near-bed rubble mound structures are often used to protect other structures such as river groins, pipelines and intake- and outfall structures for power-stations and desalination plants. From river engineering relatively extensive information is available for bed protections with currents as primary load. From coastal engineering relatively extensive information is available for low-crested rubble mound structures with waves as primary load. Information on the stability of bed protections with waves, or a combination of waves and currents, is relatively scarce. Also information on the stability of rubble mound structures with a very low-crest (*i.e.*, near-bed structures) under loading of waves and currents is scarce. Most available data concerns data related to start of damage, providing little information on damage levels related to failure of these structures. In the present study physical model tests have been performed to contribute to the understanding of relevant processes and to fill relevant gaps in the existing information on near-bed structures and bed protections.

Based on the new data and a re-analysis of existing data, several methods to predict the stability of near-bed structures have been analysed. One of these methods was found to be the most appropriate. This method was calibrated to relate the erosion of near-bed structures to a mobility parameter. It was found that for low-to-moderate currents in combination with waves, the waves dominate the stability of the rubble mound material. For waves in combination with a strong current insufficient data was available to draw firm conclusions. For the tests with a combination of waves and a low-to-moderate current the stability of the near-bed structures can be predicted without taking the influence of the current into account; the scatter related to conditions with waves in combination with a current is within the scatter for conditions with waves only.

The data-set obtained on the stability of bed protections behind near-bed structures is too small to obtain a reliable prediction method based on this data-set only. The data can however be used to verify hypotheses and numerical model results on this topic. In the present report most emphasis is put on the analysis of the data on near-bed structures. It is recommended to analyse the present data on bed protections in more detail in combination with other data and results from numerical models.

REV.	ORIGINATOR	DATE	REMARKS	REVIEW	APPROVED BY
0	M.R.A. van Gent 	Dec. 2001		G.M. Smith 	W.M.K. Tilmans 
	I. Wallast 				M.J.F. Stive 

KEYWORDS	STATUS
Granular material	<input type="checkbox"/> PRELIMINARY <input type="checkbox"/> DRAFT <input checked="" type="checkbox"/> FINAL
Near-bed structures	
Bed protection	
Scour protection	
Rubble mound structures	
Stability	
Damage levels	
Waves	
Currents	
Physical model tests	

PROJECT IDENTIFICATION: DC030204/H3804

Contents

List of Tables

List of Figures

List of Symbols

1	Introduction.....	1-1
	1.1 General.....	1-1
	1.2 Purpose of this study.....	1-1
	1.3 Outline	1-2
2	Physical model tests.....	2-1
	2.1 Test facility	2-1
	2.2 Model set-up and instrumentation	2-1
	2.3 Characteristic parameters	2-3
	2.4 Test programme	2-5
	2.5 Test results	2-6
	2.6 Discussion of test results	2-7
3	Analysis of results on near-bed structures	3-1
	3.1 Existing data-sets.....	3-1
	3.2 Prediction methods	3-2
	3.3 Discussion of prediction methods.....	3-13
4	Conclusions and recommendations.....	4-1

Acknowledgements

References

Tables

Figures

Photographs

List of Tables

In text:

- 2.1 Overview of tested configurations.
- 2.2 Overview of the test programme.
- 2.3 Mean flow velocities for conditions with waves.
- 2.4 Water depth conditions.
- 2.5 Current conditions.
- 3.1 Overview of standard deviations.

In Appendix Tables:

- T2.1 Configuration 1: Stability of bed protection.
- T2.2 Configuration 2: Stability of bed protection.
- T2.3 Configuration 3: Stability of bed protection and near-bed structure.
- T2.4 Configuration 4: Stability of near-bed structure.

List of Figures

In text:

- 2.1 Definition sketch.
- 3.1 Stability as function of $H_s/\Delta D_{n50}$; tests with waves only.
- 3.2 Stability as function of $H_s/\Delta D_{n50}$; tests with waves combined with a current.
- 3.3 Stability as function of $H_s/\Delta D_{n50}$; all tests.
- 3.4 Stability as function of Morison-parameter; tests with waves only.
- 3.5 Stability as function of Morison-parameter; tests with waves combined with a current.
- 3.6 Stability as function of Morison-parameter; all tests.
- 3.7 Stability as function of Shields-parameter; tests with waves only.
- 3.8 Stability as function of Shields-parameter; tests with waves combined with a current.
- 3.9 Stability as function of Shields-parameter; all tests.
- 3.10 Stability as function of mobility parameter; tests with waves only.
- 3.11 Stability as function of mobility parameter; tests with waves combined with a current.
- 3.12 Stability as function of mobility parameter; all tests.
- 3.13 Stability as function of mobility parameter; all tests including two extreme data-points.

In Appendix Figures:

- F2.1 Circuit of currents in the Scheldt flume.
- F2.2 Cross-section and plan view for Configuration 1.
- F2.3 Cross-section and plan view for Configuration 2.
- F2.4 Cross-section and plan view for Configuration 3.
- F2.5 Cross-section and plan view for Configuration 4.
- F2.6 Grading curves.
- F2.7 Examples of measured erosion profile (low amount of erosion).
- F2.8 Example of measured erosion profile (high amount of erosion).
- F2.9 Measured profile after Test F423 (near-bed structure).

List of Symbols

Roman letters:

A_e	: eroded area in a cross-section compared to the initial situation (m^2)
a_δ	: amplitude of the oscillatory wave motion at the bed (m)
B	: flume width (m)
B_c	: crest width (m)
c_D	: drag coefficient (-)
c_L	: lift coefficient (-)
c_M	: inertia coefficient (-)
D	: diameter (m)
D_{EQ}	: equivalent sphere diameter as the diameter ($D_{EQ} = 6 M_{50} / \pi \rho_s$) (m)
D_{n50}	: nominal diameter exceeded by 50% (based on weight) of the material (m)
D_{90}	: sieve diameter, 90% is smaller (m)
F_D	: drag force (N)
F_I	: inertial force (N)
F_L	: lift force (N)
f_w	: wave friction factor (-)
g	: gravitational acceleration (m/s^2)
H	: wave height (m)
H_s	: significant wave height of incident waves at the toe of the structure, <i>i.e.</i> $H_{1/3}$ (m)
h	: water depth at toe of structure (m)
h_c	: water depth at the crest of the near-bed structures (m)
k	: wave number $k = 2\pi/L$ (m^{-1})
k_s	: bed roughness factor (m)
k_1	: volume shape factor (-)
k_2	: area shape factor (-)
L	: wave length (m)
M_{50}	: mass of a stone exceeded by 50% of the material (kg)
N	: number of waves (-)
N_d	: number of displaced stones (-)
N_{od}	: number of displaced stones per width of one stone diameter D_{n50} (-)
n	: porosity (-)
S	: damage level (-)
s_m	: wave steepness based on the mean wave period, $s_m = 2\pi/g \cdot H_s/T_m^2$ (-)
s_{-1}	: wave steepness based on a spectral wave period, $s_{-1} = 2\pi/g \cdot H_s/T_{m-1,0}^2$ (-)
T	: wave period (s)
T_m	: mean wave period (s)
$T_{m-1,0}$: wave period based on zeroth and first negative spectral moment (s)
u_c	: velocity of the current (m/s)

- \hat{u}_δ : peak bottom velocity (m/s)
 W_s : submerged weight of a stone (N)

Greek letters:

- α : slope of the structure ($^\circ$)
 Δ : relative density $\Delta = (\rho_s - \rho) / \rho$.
 μ : angle of internal friction ($^\circ$)
 θ : mobility parameter (-)
 ρ : density of water (kg/m^3)
 ρ_s : density of rock (kg/m^3)
 σ : standard deviation (-)
 τ : shear stress (kgm/s^2)
 τ_c : shear stress due to current (kgm/s^2)
 τ_w : shear stress due to waves (kgm/s^2)
 ψ : Shields-parameter

I Introduction

I.1 General

In river and coastal engineering bed protections and near-bed rubble mound structures are often used to protect other structures such as river groins, pipelines and intake- and outfall structures for power-stations and desalination plants. Sufficiently accurate methods to predict the stability of these rubble mound structures are required for design and maintenance purposes. The present study aims for a better understanding of the relevant physical processes involved, and the translation into prediction methods. This is done based on data from existing and new physical model tests.

A wide variety of geometries of near-bed structures and bed protections exist. The present study is limited to rubble mound near-bed structures with slopes in the range of 1:1 to 1:8, and a horizontal rubble mound bed protection behind near-bed structures of this type. Near-bed structures are described as structures with a crest so low that no severe wave breaking occurs due to this structure. The relevant hydraulic boundary conditions for the above mentioned structures concern 'waves', 'currents' and 'waves in combination with currents'. To each of these three types of hydraulic loading attention is given. Most emphasis is put on 'waves' and 'waves in combination with a current', rather than on 'currents only'.

From river engineering relatively extensive information is available for bed protections with currents as primary load. From coastal engineering relatively extensive information is available for low-crested rubble mound structures with waves as primary load. Information on the stability of bed protections with waves, or a combination of waves and currents, is relatively scarce. Also information on the stability of rubble mound structures with a very low-crest (*i.e.* near-bed structures) under loading of waves and currents is scarce.

To predict the stability of near-bed structures several methods exist. The new data and existing data are used to examine these methods and to develop further the most suitable prediction method.

I.2 Purpose of this study

The purpose of this study is to gain insight into relevant physical processes related to the stability of near-bed structures and bed protections. By means of new physical model tests and re-analysis of existing data, it is aimed for to increase the accuracy and field of application of prediction methods for the stability of near-bed structures.

1.3 Outline

Chapter 2 describes the new physical model tests and the results of these tests. In Chapter 3 the analysis of the present tests and the re-analysis of existing data is described, in combination with a comparison with prediction methods for the stability of near-bed structures. Conclusions and recommendation based on the present study are given in Chapter 4.

2 Physical model tests

2.1 Test facility

The physical model tests were performed in the Scheldt-flume of WL | Delft Hydraulics ('De Voorst'). This flume has a length of 55 m, a width of 1 m and a height of 1.2 m. The facility is equipped with a wave board for generating regular/monochromatic and irregular/random waves in relatively shallow water by a translatory wave board. The on-line computer facilities for wave board control, data-acquisition and data-processing allow for direct control and computation of relevant wave characteristics. Wave energy spectra can be prescribed by using standard or non-standard spectral shapes or by prescribing specific time-series of wave trains. The wave board has active wave absorption which means that waves propagating towards the wave board are measured and that the motion of the wave board compensates for these reflected waves so that these waves do not re-reflect towards the model. In the present tests second-order wave generation and active reflection compensation is used.

The Scheldt-flume also allows for generating currents. For this purpose the facility is equipped with a maximum capacity of 120 l/s. Higher flow velocities can be generated by placing additional pump capacity. For these tests two pumps were added, each with a capacity of 20 l/s. The pumps circulate the water in a circuit as indicated in Figure F2.1 in the Appendix 'Figures'. Depending on the required water depth h the maximum mean current can be determined with (the width of the flume B is 1.0 meter):

$$u_{c-\max} = \frac{Q_{\max}}{h \cdot B} \quad (2.1)$$

In order to provide a proper inflow the main flow (maximum of 120 l/s) is conducted through a box filled with small marbles. This box has a length of about 0.5 m and secures diffusion of the water jet. The discharge is extracted at the end of the flume.

2.2 Model set-up and instrumentation

Model set-up

To study the stability of near-bed structures and the bottom protection behind such near-bed structures, four configurations have been tested. Figure 2.1 shows a definition sketch of parameters involved. Table 2.1 provides an overview of the configurations tested.

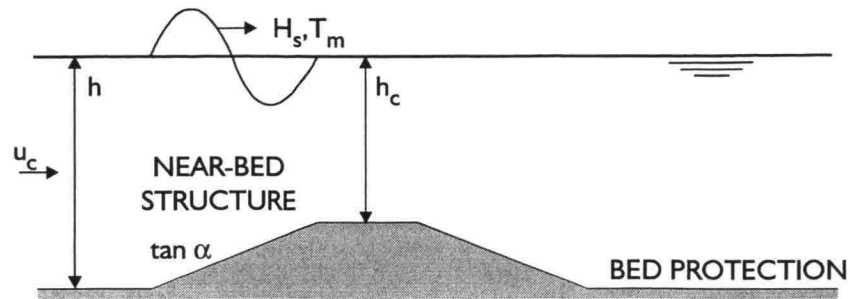


Figure 2.1 Definition sketch.

Figures F2.2-F2.5 in the Appendix ‘Figures’ show the details of Configurations 1-4. In all configurations the width of the crest was 0.125 m. For Configuration 1 and 2 the material in the near-bed structure was fixed by adding a small amount of mortar. Configurations 1 and 2 were mainly to study the bed protections; Configurations 3 and 4 were mainly performed to study the near-bed structures.

Configuration	Near-bed structure		Bed protection
	Slope	Material	Material
1	1:3	fixed	$D_{n50} = 7.2$ mm
2	1:3	fixed	$D_{n50} = 3.1$ mm
3	1:3	$D_{n50} = 7.2$ mm	$D_{n50} = 3.1$ mm
4	1:8	$D_{n50} = 3.1$ mm	$D_{n50} = 3.1$ mm

Table 2.1 Overview of tested configurations.

The bed protection of Configuration 1 and 2 stretched over 2 meters downstream of the near-bed structure. For Configuration 1 a filter layer ($D_{n50} = 2.4$ mm) with a thickness of 0.01 m was applied underneath the cover layer ($D_{n50} = 7.2$ mm) with a thickness of 0.03 m (total thickness 0.04 m). For Configurations 2-4 no filter layer was applied while the thickness of the cover layer was 0.04 m. For Configurations 3 and 4, shown in Figures F2.4 and F2.5, the same bed protection was placed on the upstream side of the near-bed structure such that a symmetric cross-section was obtained.

The grading curves of the two applied gradings for the cover layers ($D_{n50} = 3.1$ mm and 7.2 mm) and the filter material are shown in Figure F2.6. The rock density was 2650 kg/m³.

Instrumentation

An array of three wave gauges, used to determine the incident and reflected waves, was positioned at 15.5 m from the wave board (the distance between the toe of the near-bed structure and the wave board was 34.0 m for Configurations 1-3 and 33.6 m for Configuration 4). Near the structure seven wave gauges were placed, two gauges were positioned upstream of the structure, one at the toe, two at the crest, one at the downstream toe and one downstream of the structure.

In front of the structure a Velocity Current Meter (VCM) was placed at 330 mm above the bed. For one series of tests four velocity meters were positioned at the downstream toe of the structure, each one on a different vertical elevation. The exact positions of the WHM's and VCM's are indicated in Figures F2.2 to F2.5.

For the tests with waves and currents, the current was generated before starting with wave generation. Without waves the current measured upstream of the structure (VCM01) appeared to be close to 10% higher than the mean velocity obtained from $u_c = Q / (h B)$. These differences of 10% are due to vertical variations of the horizontal velocity. The velocity at VCM01 was used to check the generated mean velocity.

The measurements of the profile were made with a surface profiler. The profiler consisted of a gauge which was fastened to a computer-controlled carriage. While the carriage moved horizontally, the gauge followed the vertical level of the structure with a small wheel (with a diameter of 0.025 m) that was connected to the gauge with a spring. The gauge measured the elevation of the structure every horizontal distance of 0.004 m along the structure slope. The profile of the structure was measured along 5 rows in the longitudinal direction of the flume. With these 5 profiles an average erosion profile was determined.

The diameter of the wheel of the profiler was larger than the nominal stone diameter. Therefore, for a few tests in which a relative low amount of displaced stones occurred, it was checked whether the movement of individual stones could also be detected. After comparison of the number of displaced stones with the profiler, these results were compared with the visually counted number of displaced stones. It could be concluded that the profiler indeed provided rather accurately the number of moved stones. For tests with relatively high numbers of displaced stones, the profiler was not used to detect individual stones but to measure the reshaped profile (Configurations 2-4). The profiler measured the elevation of the structure with an accuracy of 0.001 m.

The test procedure was such that before each test the reference profile was measured. Then the profiles were measured after 1000 and after 3000 waves. Thereafter, the cover layer was repaired in order to start the subsequent test-run. Based on the differences with the reference profile the difference in elevation was computed and plotted. A number of these plots showing the difference in elevation as function of horizontal distance from the toe are presented in Figure F2.7.

2.3 Characteristic parameters

To characterise the test programme and to analyse the results use is made of a number of characteristic parameters for the waves, the current, the near-bed structure and the damage to the near-bed structure and to the bed protection.

Waves

For the wave heights of the incident waves use is made of both time-domain analysis and frequency-domain analysis. Time-domain analysis yields the significant wave height H_s , *i.e.* $H_{1/3}$, and spectral analysis the wave height H_{m0} . The wave heights in the time-domain are obtained from zero-crossings with respect to the mean water level at the corresponding position.

For the wave period numerous characteristic wave periods can be used, either based on time-domain analysis (mean wave period T_m , based on zero-crossings with respect to the mean water level) or spectral analysis. Based on spectral analysis wave periods based on moments of the wave energy spectra can be obtained. From the obtained wave energy spectra the spectral moments are computed as follows:

$$m_n = \int_0^{\infty} f^n \cdot S(f) \cdot df \quad , \quad n = \dots -4, -3, -2, -1, 0, 1, 2, \dots \quad (2.2)$$

where m_n is the n-th moment of the energy density spectrum, f the frequency and S the spectral density. Using negative moments leads to wave periods where the lower frequencies in the wave energy spectrum are relatively more important compared to the higher frequencies. Results are presented using the following wave period based on spectral moments:

$$T_{m-1,0} = \frac{m_{-1}}{m_0} \quad (2.3)$$

In the present test programme (Chapter 2) and in data from existing data-sets (Chapter 3) the shape of the wave energy spectra has not been varied. Therefore, the optimal characteristic wave period to describe the stability of near-bed structures or bed protections cannot be assessed based on these results. In this report the mean wave period T_m is used as characteristic wave period. Because other phenomena such as wave run-up, wave overtopping and stability of rock slopes can be better described using the spectral wave period $T_{m-1,0}$ this wave period is also presented as one of the output parameters.

Currents

The mean current velocity u_c is used as characteristic velocity for the velocity profile in the situation without structure (“undisturbed profile”). The mean current velocity at the crest of the near-bed structure can be calculated by using $u_{c-crest} = u_c (h_c / h)$ where h_c is the water depth above the crest and h the water depth at the toe of the structure (“undisturbed”).

Near-bed structure

The near-bed structure is characterised with the stone diameter D_{n50} (7.2 mm or 3.1 mm), the slopes ($\tan \alpha = 1:3$ or $1:8$), the water depth h_c above the crest (crest height: $h-h_c$) and the width of the crest B_c (0.125 m).

Damage

The erosion within the vertical plane was characterised with the eroded area A_e . The non-dimensional parameter characterising the eroded area is:

$$S = \frac{A_e}{D_{n50}^2} \quad (2.4)$$

For a small erosion area it might be more appropriate to use the actual number of displaced stones (N_d) or the number of displaced stones per width of one stone diameter (N_{od}), since the displacements do not lead to a single eroded area which characterises the reshaped profile. Assuming a characteristic porosity n the relation between the number of displaced stones N_d and the damage level S is as follows:

$$S = \frac{N_d \cdot D_{n50}}{(1-n) \cdot B} = \frac{N_{od}}{(1-n)} \quad (2.5)$$

where B is the width of the flume ($B=1$ m).

2.4 Test programme

A series of combinations of water levels, wave conditions and magnitude of currents was used to test the 4 earlier mentioned configurations (Table 2.1). Table 2.2 provides an overview of the conditions with waves and conditions with waves in combination with a current. For all tests with waves Jonswap-spectra were used. The wave steepness was taken constant in all tests ($s_m=0.045$ which corresponds to $s_l=0.043$).

	Configuration			Water depth h_c (m)			Wave height H_s (m)	Velocity u_c (m/s)
	Slope	D_{n50} -structure	D_{n50} -bed	0.25	0.375	0.50		
1	1:3	fixed	7.2 mm	X	X	X	0.12-0.21	0-0.41
2	1:3	fixed	3.1 mm	X			0.09-0.15	0-0.42
3	1:3	7.2 mm	3.1 mm	X	X		0.06-0.19	0-0.46
4	1:8	3.1 mm	3.1 mm	X	X		0.08-0.19	0-0.74

Table 2.2 Overview of test programme (conditions with waves and waves in combination with a current).

In Tables T2.1 to T2.4 in the Appendix ‘Tables’ the exact combinations of water levels, wave conditions and magnitude of currents are given per test-run. The naming of the test-runs in these tables is as follows:

- The first character indicates whether the test was carried out with waves only (A), only a current (V), or with a combination of waves and a current (B to F). Table 2.3 shows the mean flow velocity for the conditions with waves.

	A	B	C	D	E	F
Current (m/s)	0	0.10	0.20	0.34	0.45	0.74

Table 2.3 Mean flow velocities for conditions with waves (applied letters in naming of test-runs).

- The first digit in the naming of the tests in Tables T2.1 to T2.4 indicates the tested configuration as described in Table 2.1.
- The second digit in the name is related to the water depth above the crest (h_c) as described in Table 2.4.

	0	1	2
Water depth h_c (m)	0.50	0.375	0.25

Table 2.4 Water depth conditions (second number in naming of test-runs).

- The third digit is either related to the wave height for Series A to F, or to the magnitude of the current for Series V (Table 2.5).

	1	2	3
Current V (m/s)	0.2	0.35	0.46

Table 2.5 Current conditions (third number in naming of test-runs with currents only).

For instance, Test C221 concerns Configuration 2, a test with waves and a current of 0.2 m/s and a water depth at the crest of 0.25 m. The wave height was 0.12 m. Test V411 was a test without waves on Configuration 4, a water depth at the crest of 0.375 m, and a current of 0.2 m/s.

The tests with waves were performed for 1000 and 3000 waves. The tests with currents were run for 20 minutes. Directly after each test the relevant wave parameters, spectra and exceedance curves of the incident waves at all measurement locations were checked before the subsequent test-run was started. In addition to this, after completion of each profile measurement the results were also checked and, if necessary, corrected or repeated.

2.5 Test results

In Tables T2.1-T2.4 in the Appendix ‘Tables’ the measured wave and current conditions are presented together with the resulting damage levels. Per test-run damage numbers are given

after 1000 waves, and after a total of 3000 waves. The tables show several damage numbers. The damage is determined either by counting the number of stones, or by using the reshaped profiles. For situations with little damage (Configuration 1) the damage numbers are based on counting the number of displaced stones as follows (an example of these profile measurements with little damage is given in Figure F2.7 in the Appendix ‘Figures’):

- The number of displaced stones detected by the 5 profile measurements (N_{wheel}).
- From this value the number of displaced stones per unit width of a stone has been computed by: $N_{od} = (N_{wheel} D_{n50}) / (n_{wheel} B_{wheel})$ where B_{wheel} is the width of the wheel used to measure the (reshaped) profiles ($B_{wheel} = 0.02$ m), n_{wheel} is the number of profiles measured per cross-section (*i.e.* “number of samples”: 5).

For situations with clear reshaping of the original profile (Configurations 2-4), these reshaped profiles have been used (Figure F2.8 in the Appendix ‘Figures’ shows an example of a measured erosion profile):

- The value of S as defined by Equation 2.4. The corresponding values for N_{od} are computed using Equation 2.5.

If the first method of counting the number of displaced stones is used, the corresponding values for S are presented in Tables T2.1-T2.4 in *italic* by using an assumed porosity of $n=0.4$ in Equation 2.5. If the second method based on reshaped profiles is used, the corresponding value for N_{od} is presented in Tables T2.1-T2.4 in *italic*, also by using Equation 2.5 with $n=0.4$.

For Configuration 3 the bottom protection and the near-bed structure were not made of the same material. For some tests movement of both materials occurred. This occurred for instance for Test D321 and Test D322. For these tests two erosion areas and two damage numbers were determined. Movement of the bed protection and the near-bed structure also occurred for Tests E320-E322, but for these tests it was not possible to separate two erosion areas. Therefore, those tests have not been included in further analysis of near-bed structures in Chapter 3. Because the main damage occurred in the bed protection the damage numbers N_{od} and S presented in Table T2.3a are based on the diameter of the bed protection (*i.e.* $D_{n50} = 0.0031$ m).

Photographs were taken for the tests with Configuration 1 and Configuration 3. A selection is shown in the Appendix ‘Photographs’.

2.6 Discussion of test results

In Chapter 3 the data on the stability of the near-bed structures is analysed together with existing data on near-bed structures. Before analysing the data to study the influence of several parameters it is important to examine the information on the repeatability of the

tests. For the near-bed structure four test-conditions were performed twice (Tests A312, A313, H312, H313). The average difference between the four test-conditions with the same wave conditions and the same structure is about 20%. This means that the analysis will be associated with considerable scatter, which is not uncommon in this type of investigation. For the bed protection two test-conditions with a relatively high amount of erosion were performed twice (Tests E221, H221). The average difference between the two test-conditions with the same wave conditions and the same structure is about 4%.

The data on the bed-protection is not analysed in detail in this report. Although 30 to 40 test conditions on bed-protections were tested, this might be too low to analyse the influence of all parameters on the stability of bed protections. It is recommended to collect more data on the stability of bed protections behind near-bed structures. Together with the data from the present test programme, it might be possible to develop a method for the prediction of the stability of bed protections behind near-bed structures. Also the distances over which unstable stones are displaced is one of the relevant aspects for further analysis.

3 Analysis of results on near-bed structures

3.1 Existing data-sets

The present data set concerns data on the stability of near-bed structures and the bed protection behind these near-bed structures. In this chapter the data on the stability of near-bed structures is combined with other available data on the stability of near-bed structures under waves or waves with currents.

Other existing data-sets concern data-sets by Lomónaco (1994), Levit *et al* (1997) and Vidal *et al* (1998). Although providing valuable information, the data-sets by Levit *et al* (1997) and Vidal *et al* (1998) have not been used here since these data-sets concern tests with regular waves. Therefore, the present analysis is based on the new data-set as presented in Chapter 2 and on a re-analysis of tests by Lomónaco (1994). These two series of tests with irregular waves are performed in the same wave flume (Scheldt-flume) with the same type of instrumentation and nearly the same analysis procedure. In the tests by Lomónaco (1994) the profiles were measured at 2 cross-sections per tested structure while in the new tests 5 cross-sections per tested structure were used to assess the damage level.

The total data-set, consisting of 154 conditions with waves or waves with currents, is characterised by the following ranges for the most essential parameters:

- Slope angle ($\tan \alpha$): 1:8 - 1:1
- Crest height ($h-h_c$): 0.03 - 0.25 m
- Crest width (B_c): 0.06 - 0.25 m
- Stone diameter (D_{n50}): 3.1 - 8.3 mm
- Relative density (Δ): 1.45 - 1.7
- Number of waves (N): 1000 - 3000
- Wave height (H_s): 0.07 - 0.27 m
- Wave period (T_m): 1.1 - 2.0 s
- Wave steepness (s_m): 0.03 - 0.07
- Water depth (undisturbed) (h): 0.37 - 0.90 m
- Water depth above crest (h_c): 0.24 - 0.87 m
- Mean velocity of current (u_c): 0 - 0.74 m/s
- Non-dimensional velocity [$u_c^2/(g\Delta D_{n50})$]: 0 - 10.8
- Ratio Wave height - Water depth h (H_s/h): 0.15 - 0.51
- Ratio Wave height - Water depth h_c (H_s/h_c): 0.20 - 0.88
- Stability parameter ($H_s/\Delta D_{n50}$): 5 - 50
- Damage levels (S): 1 - 1360

In Section 3.2 this data is used for comparison with methods to predict the amount of erosion of near-bed structures. At first two data-points are excluded from the analysis because it concerns two data-points (F423) with a velocity of $u_c = 0.74$ m/s ($u_c^2/(g\Delta D_{n50}) = 10.8$) while the tests with the second largest velocity concern $u_c = 0.35$ m/s ($u_c^2/(g\Delta D_{n50}) = 2.0$) (“all tests” in this chapter refers to the data-set excluding these two extreme data-points). After performing the analysis these two data-points with a velocity of $u_c = 0.74$ m/s will be compared with the results obtained from the analysis.

3.2 Prediction methods

The parameter to be predicted is one that characterises the amount of material displaced from its original position. For rock slopes the area eroded from the original cross-section (A_e) is a common parameter for characterising the stability (e.g. Thompson and Shuttler, 1975, Broderick, 1983, or Van der Meer, 1988). Dividing this eroded area by the square of the stone diameter (D_{n50}) provides a non-dimensional parameter characterising the stability of material in near-bed structures ($S = A_e / D_{n50}^2$). For near-bed structures normally a much higher damage level can be allowed than for rock slopes. Therefore, the values for S can be much higher for near-bed structures than for rock slopes.

Data on rock slopes by Thompson and Shuttler (1975) indicated that the influence of the number of waves can be estimated using the parameter S/\sqrt{N} . This was confirmed by tests by Van der Meer (1988). Klomp and Lomónaco (1995) found a similar dependency on the number of waves for near-bed structures (based on tests by Lomónaco, 1994). Hence, this dependency on the number of waves is used here (S/\sqrt{N}).

To estimate the amount of displaced material several methods are studied. The first method is based on the stability parameter $H_s/\Delta D_{n50}$, which is a common parameter for slope protections. The second method is based on a Morison-approach where estimates of forces are used. The third method is based on the Shields-parameter, which is a common parameter for bed protections and sand beds. The fourth method uses a mobility parameter where in contrast to the Shields-parameter directly a characteristic velocity is used, rather than via an estimate of shear-stresses:

Methods:

- a) Stability number $H_s/\Delta D_{n50}$
- b) Morison-approach
- c) Shields-parameter
- d) Mobility parameter

Method A: Stability number $H_s/\Delta D_{n50}$

Figures 3.1-3.3 show the parameter S/\sqrt{N} as function of the stability parameter $H_s/\Delta D_{n50}$. Figure 3.1 shows the data with waves only. Figure 3.2 shows the data with waves in combination with a current and Figure 3.3 shows all data.

The data shows considerable scatter but this is not uncommon for stability of rock; the scatter is not significantly larger than for rock slopes. There is however a sub-set of tests with a distinct deviation from the main trend [tests with a 1:3 slope, a diameter of $D_{n50}=8.3$ mm, $(h-h_c)/D_{n50}=30$]. This raises doubts on the suitability of the parameter $H_s/\Delta D_{n50}$ for this purpose. Although the parameter $H_s/\Delta D_{n50}$ does not take into account currents, the test results with waves in combination with a current appear to be within the scatter for tests with waves only: If the parameter $H_s/\Delta D_{n50}$ is used, the influence of currents does not need to be taken into account separately, for currents in the applied range of velocities [$u_c^2/(g\Delta D_{n50}) < 2$].

A prediction method based on the parameter $H_s/\Delta D_{n50}$ could be of the following shape:

$$S = c_0 \left(\frac{H_s}{\Delta D_{n50}} \right)^{c_1} N^{0.5} \quad (3.1)$$

Using $c_0 = 5 \cdot 10^{-5}$ and $c_1 = 3$ leads to a standard deviation between the value of S/\sqrt{N} from Equation 3.1 and the data for conditions with waves only of $\sigma = 2.35$. If all tests, including those with currents, are taken into account this standard deviation is $\sigma = 2.10$. Figure 3.3 shows Equation 3.1 in combination with the test results.

Method B: Morison-approach

Stability formulae based on the parameter $H_s/\Delta D_{n50}$ relate the stability to parameters which characterise the wave field, without estimating flow properties like velocities and accelerations near the stones. For this purpose a Morison-type of expression (Morison *et al.*, 1950) can be used, see for instance Kobayashi and Otta (1987) or Tørum (1992). In this approach forces are estimated based on velocities and accelerations. In addition, information on possible failure mechanisms and forces causing damage is needed. Often failure mechanisms referred to as *rolling*, *sliding* or *lifting* are distinguished. For bed protections or structures where reshaping is allowed also the new positions of unstable stones is of interest. The latter is not studied here, but for applications on berm breakwaters or gravel beaches reference is made to Van Gent (1995), where this reshaping is modelled numerically.

Three forces resulting from the hydrodynamic loads are distinguished; the drag force acting parallel to the slope in the direction of the velocity, the inertial force acting parallel to the slope and the lift force acting perpendicular to the slope. For the drag force and the inertial force expressions similar to those in the Morison equation can be used. The lift force is the

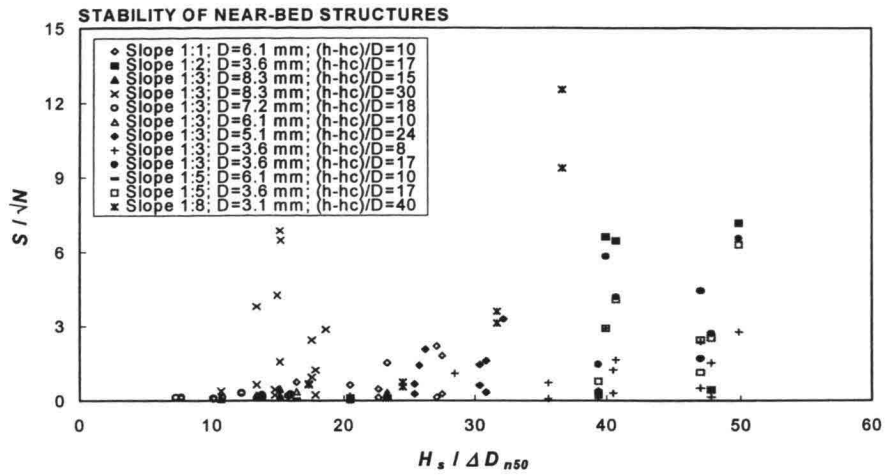


Figure 3.1 Stability as function of $H_s / \Delta D_{n50}$; tests with waves only.

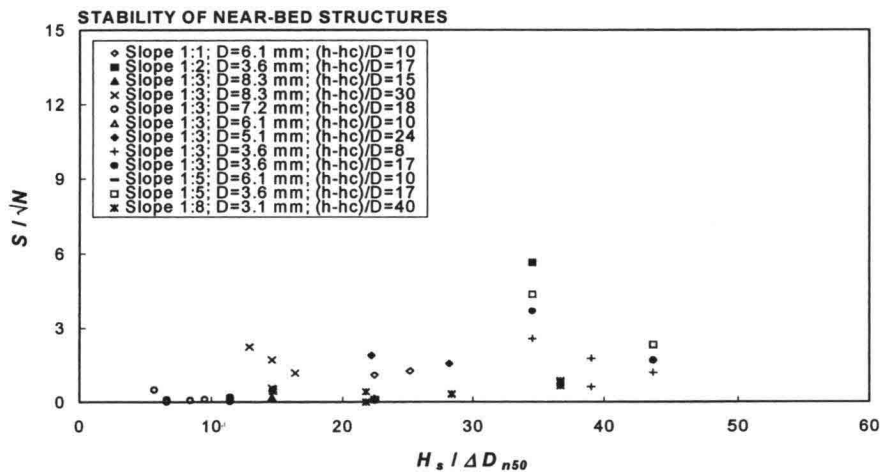


Figure 3.2 Stability as function of $H_s / \Delta D_{n50}$; tests with waves combined with a current.

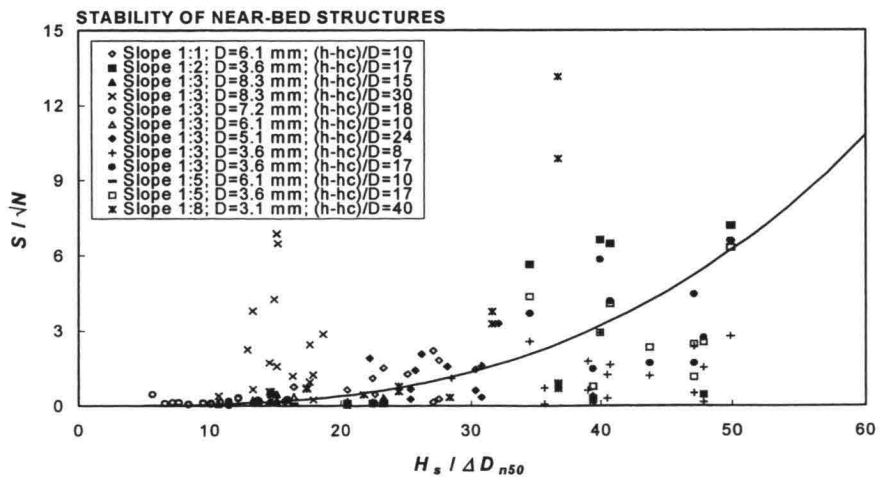


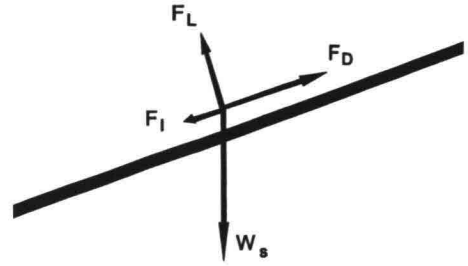
Figure 3.3 Stability as function of $H_s / \Delta D_{n50}$; all tests.

most difficult one to determine. Often, the assumption that the lift force is proportional to the squared velocity and the squared diameter of the stone is used.

$$F_D = \frac{1}{2} \rho c_D k_2 D^2 u |u| \quad (3.2)$$

$$F_I = \rho c_M k_1 D^3 \frac{Du}{Dt} \quad (3.3)$$

$$F_L = \frac{1}{2} \rho c_L k_2 D^2 u^2 \quad (3.4)$$



Forces on a stone on an upward slope.

where the acceleration Du/Dt is approximated by $\partial u/\partial t$; c_D , c_M , c_L are the drag coefficient, the inertia coefficient and the lift coefficient respectively; k_1 and k_2 are the volume shape factor and the area shape factor respectively. With the area shape factor k_2 the actual projected area in the flow direction can be incorporated. Since a stone in a bed or slope protection is partially sheltered by other stones, the actual projected area is smaller than for a single stone in a flow. The sheltering effect has not been incorporated separately and therefore affects the values of the coefficients. For spheres, the value for k_2 is $\pi/4$ since the projected area, neglecting the sheltering effect, is $\pi/4 D^2$. The volume shape factor k_1 is $\pi/6$ for spheres since its volume is equal to $\pi/6 D^3$. For stones slightly higher values must be used: $k_1=0.66$ and $k_2=0.9$ were used here. A constant stone diameter is taken, while the equivalent sphere diameter D_{EQ} is used as the characteristic stone size ($D_{EQ} \approx 1.24 \cdot D_{n50}$).

The submerged weight is often taken as the counter-acting force, although occasionally other counteracting forces have been proposed, see for instance Brandtzaeg and Tørum (1966). The submerged weight acts vertically and can be written as (ρ_s represents the density of the rock material):

$$W_s = (\rho_s - \rho) g k_1 D^3 \quad (3.5)$$

Several concepts can be used for initiation of movement. For the near-bed structures where damage is often initiated at the rear side of the structure, stability criteria for a stone on the downward slope instead of on upward slope are regarded. The stability criteria for the phenomena referred to as *lifting* and *sliding* can respectively be expressed by:

$$F_L \leq W_s \cos \alpha \quad (3.6)$$

$$(F_D + F_I + W_s \sin \alpha) \leq \tan \mu (W_s \cos \alpha - F_L) \quad (3.7)$$

where μ denotes the angle of internal friction and α the local slope angle. The phenomenon referred to earlier as *rolling* can be assumed to occur if both stability conditions are not satisfied.

The ratio of loading and resistance to *lifting* is:

$$\frac{F_L}{\cos \alpha W_s} \quad (3.8)$$

The ratio of loading and resistance to *sliding* is:

$$\frac{F_D + F_I + \tan \mu F_L + W_s \sin \alpha}{\tan \mu \cos \alpha W_s} \quad (3.9)$$

Tørum (1992) found a value of $c_D = 0.35$ for a sheltered non-moving stone in a slope of a berm breakwater. This value has been used here. Since the lift forces are in the same order of magnitude while almost no experimental data on this coefficient is available, the same values is used here for the lift coefficient ($c_L = 0.35$). Here, the inertial force is neglected because for the small material used on near-bed structures this force can be neglected compared to the lift and drag forces. For the angle of internal friction 45° ($\tan \mu = 1$) is used for all material.

To estimate a characteristic velocity the peak bottom velocity \hat{u}_δ at the crest is used. This velocity is estimated based on linear wave theory for the situation as if there were no variations in water depth:

$$\hat{u}_\delta = \frac{\pi H}{T} \frac{1}{\sinh kh_c} \quad (3.10)$$

where h_c is the depth at the crest of near-bed structures and k the wave number ($k = 2\pi/L$ see footnote¹). For the characteristic wave height and characteristic wave period, H_s and T_m are used respectively in Equation 3.10. The influence of a constant flow added to the wave field is neglected by choosing this characteristic velocity.

If one uses the ratio of loading and resistance to *lifting*, a method similar to the one described later on is described: The method based on a mobility parameter (Method D). A prediction formula based on the resistance to *lifting* reads:

$$S = c_0 \left(\frac{F_L}{\cos \alpha W_s} \right)^{c_1} N^{0.5} = c_0 \left(\frac{0.5 k_2 c_L}{\cos \alpha k_1} \frac{u^2}{g \Delta D_{n50}} \right)^{c_1} N^{0.5} \quad (3.11)$$

Using $c_0 = 25$ and $c_1 = 3$ leads to a standard deviation between the value of S/\sqrt{N} from Equation 3.11 and the data for conditions with waves only of $\sigma = 1.61$. If all tests, including those with currents, are taken into account this standard deviation is $\sigma = 1.59$.

If one uses the ratio of loading and resistance to *sliding*, the prediction formula becomes:

$$S = c_0 \left(\frac{F_D + \tan \mu F_L + W_s \sin \alpha}{\tan \mu \cos \alpha W_s} \right)^{c_1} N^{0.5} \quad (3.12)$$

¹ The wave length can be approximated by L_2 without the use of an iterative solver: $L_0 = gT^2/2\pi$, $L_1 = L_0 [1 - \exp(-(2\pi d/L_0)^{1.25})]^{0.4}$ and $L_2 = L_1 [(Q/\cosh Q)^2 + Q \tanh Q] / [(Q/\cosh Q)^2 + 2\pi d/L_0]$ where $Q = 2\pi d/L_1$ in which d is the local water depth (relative error $< 3 \cdot 10^{-5}$; method by G. Klopman).

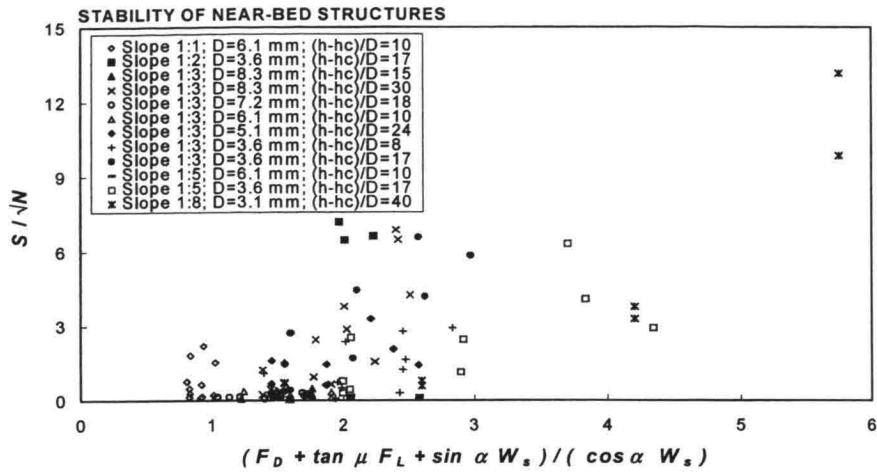


Figure 3.4 Stability as function of Morison-parameter; tests with waves only.

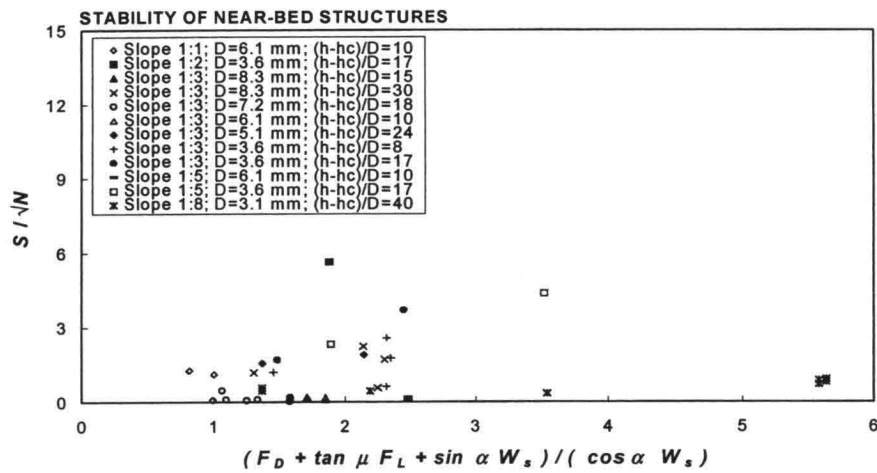


Figure 3.5 Stability as function of Morison-parameter; tests with waves combined with a current.

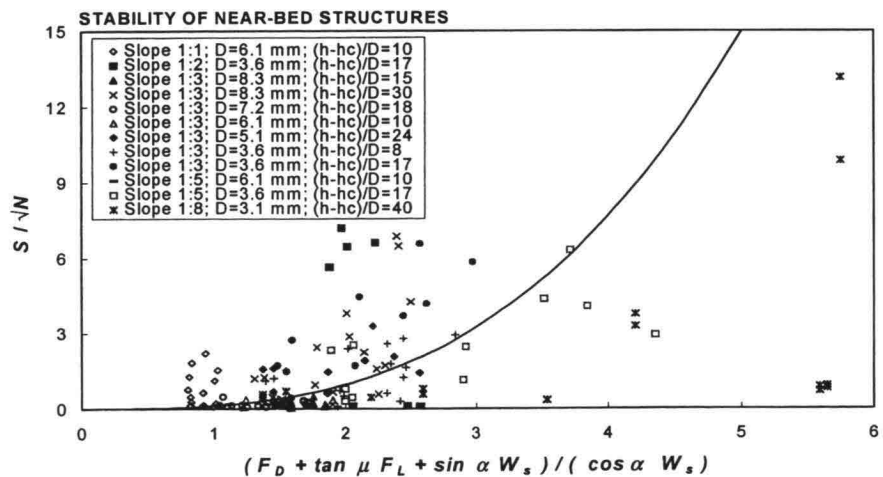


Figure 3.6 Stability as function of Morison-parameter; all tests.

Using $c_0 = 0.12$ and $c_l = 3$ leads to a standard deviation between the value of S/\sqrt{N} from Equation 3.12 and the data for conditions with waves only of $\sigma = 2.42$. If all tests, including those with currents, are taken into account this standard deviation is $\sigma = 3.94$.

Figures 3.4-3.6 show the parameter S/\sqrt{N} as function of the parameter given in Equation 3.9. Figure 3.4 shows the data with waves only, Figure 3.5 shows the data with waves in combination with a current and Figure 3.6 shows all data (waves and waves in combination with a current) in combination with Equation 3.12.

The data shows again considerable scatter. Although the characteristic velocity (Equation 3.10) does not take into account currents, most test results with waves in combination with a current appear to be within the scatter for tests with waves only. This indicates that the influence of currents does not need to be taken into account separately, for currents in the applied range of velocities [$u_c / \hat{u}_\delta < 2.2$ for $0.15 < \hat{u}_\delta^2 / (g\Delta D_{n50}) < 3.5$].

Method C: Shields-parameter

The Shields-parameter is a non-dimensional form of the bed shear stress, which is often used in combination with a critical shear stress (Shields-criterion):

$$\psi = \frac{\tau}{(\rho_s - \rho) g D} \quad (3.13)$$

For the situation with waves only a characteristic bed shear stress (τ_w) can be estimated based on Jonsson (1966):

$$\tau_w = \frac{1}{2} \rho f_w u^2 \quad (3.14)$$

This is an instantaneous bed shear stress. Averaging over a half a wave cycle yields a time-averaged bed shear stress where the characteristic velocity is the peak bottom velocity \hat{u}_δ (Equation 3.10 is used here):

$$\bar{\tau}_w = \frac{1}{4} \rho f_w \hat{u}_\delta^2 \quad (3.15)$$

For the wave friction factor f_w Kamphuis (1987) obtained the following expression:

$$f_w = 0.4 \left(\frac{a_\delta}{k_s} \right)^{-0.75}, \text{ for } \frac{a_\delta}{k_s} < 100 \quad (3.16)$$

using $k_s = 2 D_{90}$ (here: $D_{90} = 1.4 D_{n50}$) for the bed roughness and linear wave theory for the amplitude of the oscillatory horizontal wave motion at the bed (a_δ):

$$a_{\delta} = \frac{\hat{u}_{\delta} T}{2\pi} \quad (3.17)$$

For the characteristic wave period the mean wave period T_m is used in Equation 3.17. Figure 3.7 shows the parameter S / \sqrt{N} as function of the Shields-parameter where for the characteristic shear stress Equation 3.14 is used in combination with Equation 3.10 for the characteristic velocity.

For a current in combination with waves the effects of the current on the bed shear stress and on the bed roughness can be accounted for. This can be done by for instance using the average shear stress (averaged over a half a wave cycle) as characteristic bed shear stress:

$$\bar{\tau}_{cw} = \tau_c + \frac{1}{2} \tau_w = \tau_c + \bar{\tau}_w \quad (3.18)$$

However, taking into account the current in the bed shear stress does for this application not lead to an improvement. In Figure 3.8 the data on waves in combination with a current is shown, where the bed shear stress is computed using Equation 3.14, neglecting the contribution of the current. Introducing a contribution of the current to the bed shear stress would result in a shift of the data to higher values of the Shields-parameter, and consequently a shift out of the region with data on conditions with waves only (Figure 3.7). Similar to the previously discussed methods this indicates that the influence of currents does not need to be taken into account separately, for currents in the applied range of velocities [$u_c / \hat{u}_{\delta} < 2.2$ for $0.15 < \hat{u}_{\delta}^2 / (g\Delta D_{n50}) < 3.5$].

A prediction method based on the Shields-parameter (Equations 3.10, 3.13, 3.14, 3.16 and 3.17) could be of the following shape:

$$S = c_0 \psi^{c_1} N^{0.5} \quad (3.19)$$

Using $c_0 = 4 \cdot 10^5$ and $c_1 = 5$ leads to a standard deviation between the value of S / \sqrt{N} from Equation 3.19 and the data for conditions with waves only of $\sigma = 2.04$. If all tests, including those with currents, are taken into account the standard deviation is $\sigma = 2.10$. These standard deviations are smaller than for Method A based on the stability number $H_s / \Delta D_{n50}$. For conditions with waves only the standard deviation is similar to the one for Method B based on the Morison-approach (“sliding”), and for all conditions, including those with currents, smaller than the one for Method B. Figure 3.9 shows Equation 3.19 in combination with all test results.

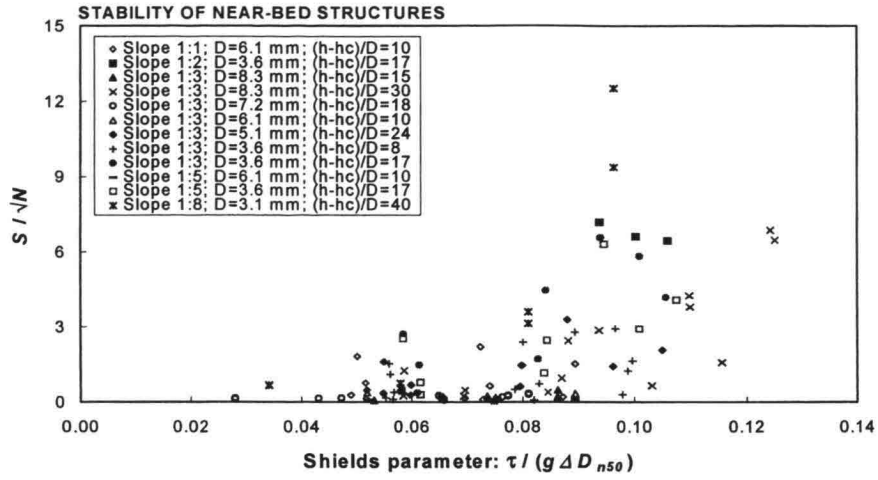


Figure 3.7 Stability as function of Shields-parameter; tests with waves only.

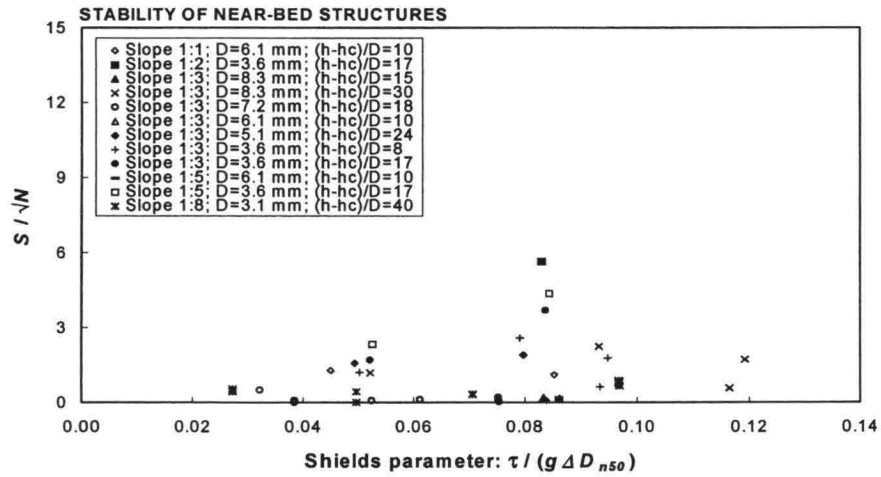


Figure 3.8 Stability as function of Shields-parameter; tests with waves combined with a current.

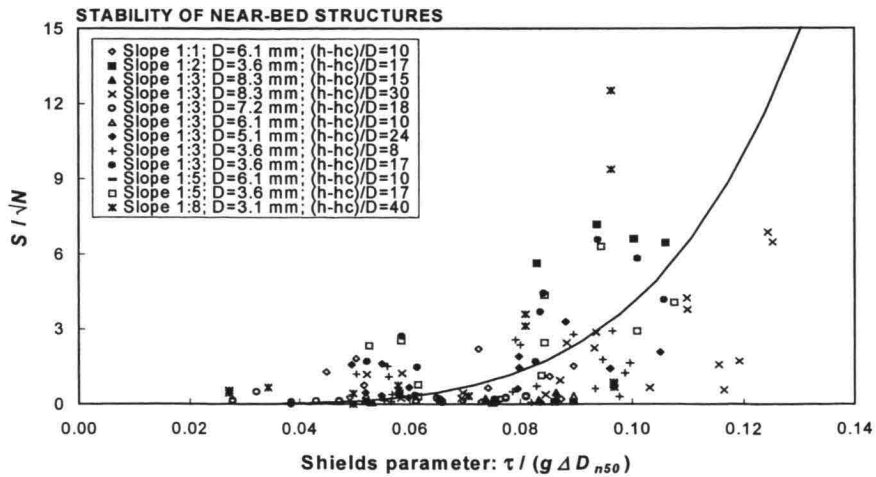


Figure 3.9 Stability as function of Shields-parameter; all tests.

Method D: Mobility parameter

The Shields-parameter (Equation 3.13) concerns a non-dimensional form of the bed shear stress, where use is made of estimates of the a characteristic velocity and a wave friction factor (f_w). The latter requires expressions for the bed roughness (k_s) and a characteristic amplitude of the oscillatory horizontal wave motion at the bed (a_δ). If the expressions for f_w , k_s and a_δ do not increase the accuracy of the predictions, a method which only uses only a characteristic velocity might be more appropriate. This yields the following mobility parameter:

$$\theta = \frac{u^2}{g \Delta D_{n50}} \quad (3.20)$$

where for the characteristic velocity the peak bottom velocity \hat{u}_δ at the crest is used (Equation 3.10).

Figures 3.10-3.12 show the parameter S/\sqrt{N} as function of the mobility parameter (Equation 3.20 using Equation 3.10). Figure 3.10 shows the data with waves only. Figure 3.11 shows the data with waves in combination with a current and Figure 3.12 shows all data (waves and waves in combination with a current).

The data shows again considerable scatter but less than for the previously discussed methods. Although the mobility parameter (Equations 3.20 and 3.10) does not take into account currents, the test results with waves in combination with a current appear to be within the scatter for tests with waves only: If the mobility parameter from Equations 3.20 and 3.10 are used, the influence of currents does not need to be taken into account separately for currents, in the applied range of velocities [$u_c/\hat{u}_\delta < 2.2$ for $0.15 < \hat{u}_\delta^2/(g \Delta D_{n50}) < 3.5$].

A prediction method based on this mobility parameter could be of the following shape:

$$S = c_0 \theta^{c_1} N^{0.5} \quad (3.21)$$

Figure 3.12 shows Equation 3.21 with $c_0 = 0.2$ and $c_1 = 3$, using H_s and T_m in Equation 3.10. The main trend in the data is clear and there is a relatively low amount of scatter. Nevertheless, the deviations from this trend are still large. This is expected to be partly due to the rough estimate of the characteristic velocity. Using $c_0 = 0.2$ and $c_1 = 3$ leads to a standard deviation between the value of S/\sqrt{N} from Equation 3.21 and the data for conditions with waves only of $\sigma = 1.54$. If all tests, including those with currents, are taken into account this standard deviation is $\sigma = 1.58$. These standard deviations are smaller than those obtained from previously discussed methods. This will be discussed further in the following section.

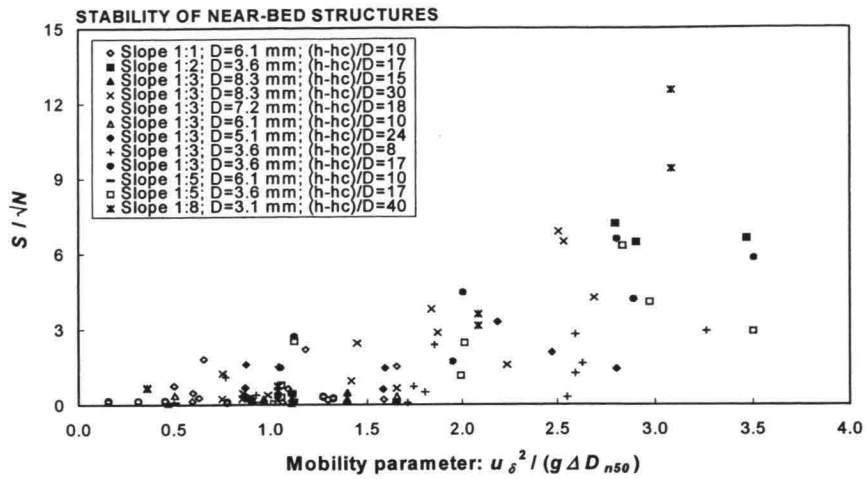


Figure 3.10 Stability as function of mobility parameter; tests with waves only.

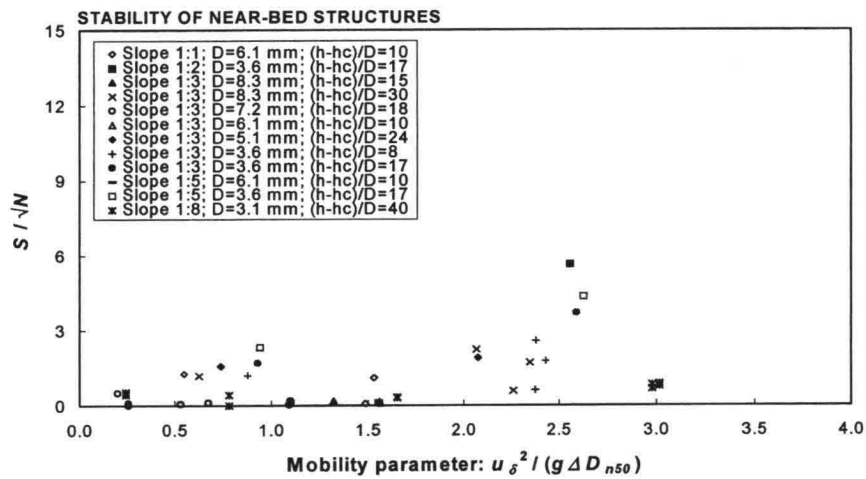


Figure 3.11 Stability as function of mobility parameter; tests with waves combined with a current.

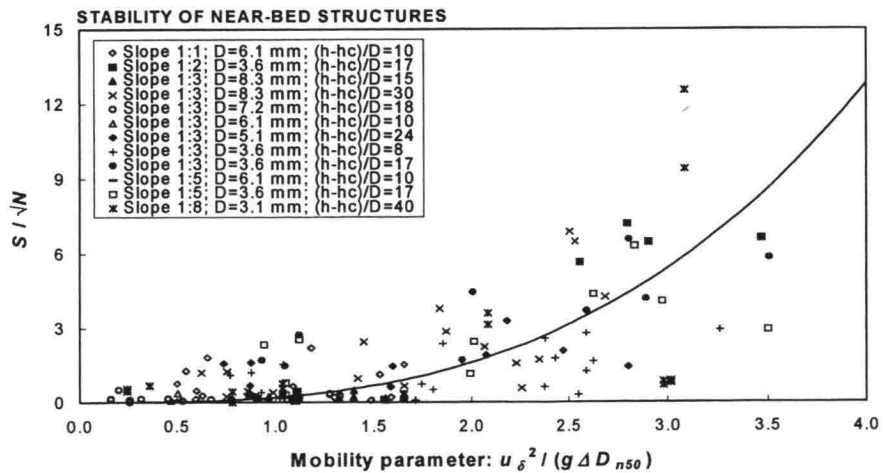


Figure 3.12 Stability as function of mobility parameter; all tests.

3.3 Discussion of prediction methods

To compare the different prediction methods use is made of the presented figures and the standard deviations between the formulae and the data (S/\sqrt{N}). These standard deviations are summarised in Table 3.1.

Figures 3.1-3.12 and Table 3.1 indicate that the method based on the mobility parameter (Equation 3.20 using Equation 3.10 for a characteristic velocity) and the method based on the failure mechanism “lifting” lead to the best predictions. The methods based on the stability number $H_s/\Delta D_{n50}$, the method based on the failure mechanism “sliding” (Morison-approach), and the method based on the Shields-parameter lead to a lower accuracy. Nevertheless, for all methods the deviations between the test results and the predictions can be considerable: The scatter is large for all methods.

Method	f (parameters)	σ - waves only	σ - all data
A Stability number	$f(N, H_s, D_{n50}, \Delta)$	2.35	2.10
B Morison-approach:	sliding $f(N, H_s, T_m, D_{n50}, \Delta, h_c, \tan \alpha)$	2.42	3.94
	lifting $f(N, H_s, T_m, D_{n50}, \Delta, h_c, \tan \alpha)$	1.61	1.59
C Shields-parameter	$f(N, H_s, T_m, D_{n50}, \Delta, h_c)$	2.04	2.10
D Mobility parameter	$f(N, H_s, T_m, D_{n50}, \Delta, h_c)$	1.54	1.58

Table 3.1 Overview of standard deviations.

Comparing the methods based on the mobility parameter (Equation 3.21 using Equation 3.10 for a characteristic velocity) and the method based on the failure mechanism “lifting” (Equation 3.11) shows that they result in similar expressions. With k_1 and k_2 being constant factors and c_L being a coefficient for which it is difficult to obtain an accurate estimate (Tørum, 1992), the slope angle is the only extra parameter in Equation 3.11 compared to the mobility parameter. This extra parameter does however not lead to an improvement of the predictions: The standard deviations are nearly the same. Therefore, preference is given to the more simple method based on the mobility parameter (Method D). Table 3.1 also shows the parameters that are taken into account in the various methods. Comparison of the standard deviations indicate that the number of waves (N), the wave height (H_s), the wave period (T_m), the stone diameter (D_{n50}), the relative density (Δ) and the water depth above the crest (h_c) are the six most important parameters. The velocity of the current (u_c), the slope of the near-bed structure ($\tan \alpha$), the water depth in front of the structure (h) and the crest width (B_c) were varied in the tests but seem to be less important.

The mobility parameter on its own does not show its physical background. However, the similarity with the method based on a balance of forces (failure mechanism “lifting” with the influence of the slope angle neglected) and the method based on a characteristic shear-stress (Shields-parameter, with in fact a constant wave friction factor) provide to some extent a physically sound base for the use of the mobility parameter.

The conditions in the available data-set with currents in combination with waves concern conditions with a limited mean velocity of the current [$u_c < 0.35$ m/s and $\hat{u}_c^2 / (g \Delta D_{n50}) < 2$]. Although there are effects of the currents, these effects are small compared to the scatter in the data-set. Therefore, it is considered appropriate to neglect the influence of currents for conditions in the present data-set. As mentioned in Section 3.1 two test results were at first excluded from the analysis since it concerned conditions with a combination of waves and a relatively strong current [$u_c = 0.74$ m/s; $u_c^2 / (g \Delta D_{n50}) = 10.8$; $u_c / \hat{u}_\delta = 1.4$; $\hat{u}_\delta^2 / (g \Delta D_{n50}) = 5.2$]. Using these two data-points in the analysis shows that for “Method B - lifting”, “Method C - Shields-parameter” and “Method D - Mobility parameter” these two data-points are close to the curves describing the main trends through the data-points (Equations 3.11, 3.19 and 3.21). For the other methods these two data-points deviate considerably from the main trend through all data-points. Figure 3.13 shows all data including these two data-points for Method D (Mobility parameter). The number of tests with strong currents is limited in the present data-set. Therefore, neglecting the effects of currents for conditions outside the mentioned range [$u_c < 0.35$ m/s and $\hat{u}_c^2 / (g \Delta D_{n50}) < 2$] cannot be justified based on the present analysis.

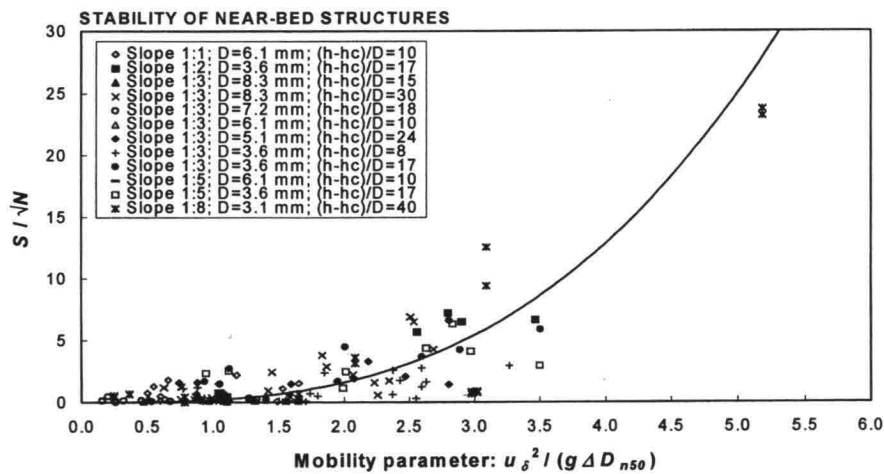


Figure 3.13 Stability as function of mobility parameter; all tests including two extreme data-points.

One of the observations in the tests was that adding a current to a wave field does not systematically lead to an increase of the damage to near-bed structures compared to the situation with the wave field only. It is expected that adding a current to the wave field increases the mean velocity at the bottom and increases time-averaged shear-stresses and drag and lift forces. In the range of the analysed test conditions this seems to be counteracted by other phenomena. It is expected that it is rather important whether the velocity at the bottom changes direction within a wave cycle for a situation with waves in combination with a current. If there is no change in the direction of the velocity at the bottom the material is expected to be more stable. Other effects of the presence of a current that are expected to play a role are the changes in the wave motion and other time-

dependent flow patterns around the structure. This indicates that changes in the time-derivative of the velocity could be relatively important. It is recommended to study the flow characteristics around near-bed structures more in detail to obtain more information on the interaction between waves, a current and the structural response.

4 Conclusions and recommendations

Based on the investigations described in this report the following conclusions and recommendations can be given:

Conclusions:

- By performing physical model tests a data-set was created on rubble mound near-bed structures with bed protections behind these structures. The data contains conditions with waves and waves in combination with a current. The data-set on near-bed structures is large compared to the data on the bed protections. In this report, analysis was focussed on near-bed structures.
- For near-bed structures four methods have been used to estimate the amount of damage. The method based on the stability number $H_s/\Delta D_{n50}$ appeared to lead to a large amount of scatter. The method based on a mobility parameter appeared to be the most suitable one. Based on the present data-set and a re-analysis of existing data the following simple formula was obtained:

$$S = 0.2 \theta^3 N^{0.5} \quad (4.1)$$

with

$$\theta = \frac{u^2}{g \Delta D_{n50}} \quad (4.2)$$

and

$$u = \frac{\pi H_s}{T_m} \frac{1}{\sinh kh_c} \quad (4.3)$$

where S is a measure for the amount of damage, N is the number of waves, θ is the mobility parameter and u a characteristic velocity.

- The conditions in the available data-set with currents in combination with waves concern conditions with a limited mean velocity of the currents [$u_c/\hat{u}_\delta < 2.2$ for $0.15 < \hat{u}_\delta^2/(g\Delta D_{n50}) < 3.5$]. Although there are effects of the currents, these effects are small compared to the scatter in the data-set. Therefore, it is considered appropriate to neglect the influence of currents for conditions in the present data-set. However, it is likely that for larger velocities of currents these effects cannot be neglected. Therefore, neglecting the effects of currents for conditions outside the range of the present data-set cannot be justified based on the present analysis.

Recommendations:

- The present study provides insight into the stability of near-bed structures and provides new data for near-bed structures and bed protections. The analysis was mainly focussed on near-bed structures. It is recommended to collect more data on the stability of bed protections behind near-bed structures. Together with the data from the present test programme, it might be possible to develop a method for the prediction of the stability of bed protections behind near-bed structures. The distances over which unstable stones are displaced is one of the relevant aspects for further analysis.
- The present study yields a prediction method for the stability of near-bed structures. The scatter around the main trend is rather large, although this is not uncommon for rubble mound structures under wave attack. Nevertheless, it is recommended to take the amount of scatter into account when applying the prediction method. More fundamental research could lead to more insight into the phenomena leading to this scatter.
- The results will to some extent be affected by scale effects. It would be valuable to check whether these scale effects are negligibly small by performing some tests on a larger scale.
- Flow patterns around near-bed structures and bed-protections are affected by changes in the profile due to damage. In the applied methods to predict damage to near-bed structures, the effects of these changes are neglected. It is recommended to study the effects of these changes more in detail.
- It is recommended to study the flow characteristics around near-bed structures more in detail. Especially the interaction between waves and a relatively strong current, and the effects of the combination of waves and a current on the stability of near-bed structures, require further attention to understand the stability of near-bed structures.
- To understand the relevant processes and to predict the stability of stones in near-bed structures and bed protections, it is recommended to study whether a method can be obtained where a) the motion of water is computed in detail, and b) the stability and transport of individual stones is related to the instant motion of water.

Acknowledgements

Motivation and development of this work have been stimulated in the context of the Delft Cluster project 'Behaviour of granular material' (In Dutch: 'Gedrag van grofkorrelig materiaal'); Project 03-02-04.

References

- Brandtzaeg, A. and A. Tørum (1966), *A simple mathematical model of wave motion on a rubble mound breakwater front*, Proc. ICCE'66, Vol.2, pp.977-989, Tokyo.
- Broderick, L.L. (1983), *Riprap stability a progress report*, ASCE, Proc. Conference on Coastal Structures '83, pp.320-330.
- Jonsson, I.G. (1966), *Wave boundary layers and friction factors*, ASCE, Proc. ICCE'66, pp.127-148.
- Kamphuis, J.W. (1987), *Friction factor under oscillatory waves*, ASCE, J. of Waterways and Harbour Division, Vol.101, pp.135-144.
- Klomp, W.H.G. and P. Lomónaco (1997), *Pipeline cover stability*, Proc. 5th Int. Offshore and Polar Engineering Conference (ISOPE), pp.15-22, The Hague, The Netherlands.
- Kobayashi, N. and A.K. Otta (1987), *Hydraulic stability analysis of armour units*, J. of Waterway, Port, Coastal and Ocean Engineering, ASCE, Vol.113, No.2, pp.171-185.
- Levit, M., M.R.A. van Gent and W.W. Massie (1997), *Stability of pipeline covers under waves and currents*, Proc. 8th Int. Conf on the Behaviour of Offshore Structures (BOSS'97), Vol.1, pp.195-210, Delft.
- Lomónaco, P. (1994), *Design of rock cover for underwater pipelines*, M.Sc.-thesis International Institute for Infrastructural, Hydraulic and Environmental Engineering, Delft.
- Lomónaco, P. and W.H.G. Klomp (1997), *Pipeline cover damage assessment*, Proc. 8th Int. Conf on the Behaviour of Offshore Structures (BOSS'97), Vol.1, pp.179-193, Delft.
- Morison, J.R., M.P. O'Brien, J.W. Johnsen and S.A. Schaff (1950), *The forces exerted by surface waves on piles*, Petrol. Trans. AIIME, Vol.189, pp.149-154.
- Thompson, D.M. and R.M. Shuttler (1975), *Riprap design for wind wave attack; a laboratory study in random waves*, HRS Wallingford, Report EX 707.
- Tørum, A (1992), *Wave induced water particle velocities and forces on an armour unit on a berm breakwater*, MAST-G6S report and Report STF60-A92104, Norwegian Hydrotechnical Laboratory-Trondheim, Norway.
- Van der Meer, J.W. (1988), *Rock slopes and gravel beaches under wave attack*, Ph.D. thesis Delft University of Technology, also Delft Hydraulics publication No.396.
- Van Gent, M.R.A. (1995), *Wave interaction with permeable coastal structures*, Ph.D.-thesis, Delft University of Technology, ISBN 90-407-1182-8, Delft University Press, Delft.
- Vidal, C., Í.J. Losada, F.L. Martín (1998), *Stability of near-bed rubble mound structures*, ASCE, Proc. ICCE 1998, Vol. 2, pp.1730-1743, Copenhagen.

Tables

Stability of bed protection										
No.	Water depth		Velocity	Waves					Damage	
	h	h_{crest}	u_c	$H_{1/3}$	H_{m0}	T_m	$T_{m-1,0}$	N_{waves}	N_{od}	S
A101	0.665	0.500	0	0.138	0.140	1.30	1.43	1000	4.4	7.4
								3000	2.0	3.3
A102	0.665	0.500	0	0.177	0.181	1.48	1.65	1000	1.9	3.2
A103	0.665	0.500	0	0.209	0.213	1.60	1.84	1000	1.6	2.6
								3000	2.3	3.8
A112	0.540	0.375	0	0.170	0.172	1.50	1.67	1000	2.3	3.8
								3000	1.9	3.2
A113	0.540	0.375	0	0.192	0.198	1.59	1.87	1000	2.7	4.5
								3000	2.1	3.6
A122	0.415	0.250	0	0.146	0.154	1.53	1.71	1000	3.2	5.3
A123	0.415	0.250	0	0.158	0.170	1.67	1.89	1000	3.2	5.3
C122	0.415	0.250	0.21	0.131	0.139	1.48	1.68	1000	4.3	7.2
								3000	4.6	7.6
C123	0.415	0.250	0.22	0.146	0.154	1.58	1.85	1000	3.5	5.9
								3000	5.4	9.0
D122	0.415	0.250	0.31	0.122	0.131	1.46	1.68	1000	4.3	7.2
E122	0.415	0.250	0.41	0.122	0.127	1.48	1.67	1000	19.2	32.0
								3000	21.6	36.0

Table T2.1 Configuration 1: Stability of bed protection;
 Near-bed structure: fixed bed, slope 1:3;
 Bed protection: $D_{n50} = 7.2$ mm.

Stability of bed protection										
No.	Water depth		Velocity	Waves					Damage	
	h	h_{crest}	u_c	$H_{1/3}$	H_{m0}	T_m	$T_{m-1,0}$	N_{waves}	N_{od}	S
A221	0.415	0.250	0	0.121	0.128	1.33	1.46	1000	8.8	14.7
A222	0.415	0.250	0	0.146	0.153	1.49	1.70	1000	5.5	9.2
C221	0.415	0.250	0.20	0.106	0.111	1.26	1.48	1000	5.2	8.6
C222	0.415	0.250	0.20	0.129	0.136	1.44	1.68	1000	6.1	10.1
D222	0.415	0.250	0.32	0.119	0.127	1.41	1.68	1000	5.7	9.5
								3000	19.5	32.5
E221	0.415	0.250	0.42	0.094	0.098	1.32	1.47	1000	88.0	146.6
								3000	243.0	404.9
H221	0.415	0.250	0.42	0.094	0.098	1.32	1.47	1000	80.8	134.7
=E221								3000	241.8	403.0
V223	0.415	0.250	0.42						1.4	2.4

Table T2.2 Configuration 2: Stability of bed protection;
 Near-bed structure: fixed bed, slope 1:3;
 Bed protection: $D_{n50} = 3.1$ mm.

Stability of bed protection										
No.	Water depth		Velocity	Waves					Damage	
	h	h_{crest}	u_c	$H_{1/3}$	H_{m0}	T_m	$T_{m-1,0}$	N_{waves}	N_{od}	S
D321	0.375	0.250	0.35	0.098	0.104	1.30	1.45	1000	11.1	18.5
								3000	11.7	19.5
D322	0.375	0.250	0.35	0.122	0.129	1.46	1.67	1000	4.8	8.0
								3000	12.5	20.8
E320	0.375	0.250	0.46	0.064	0.068	1.12	1.21	1000	65.8	109.6
								3000	200.3	333.9
E321	0.375	0.250	0.46	0.094	0.098	1.31	1.46	1000	83.9	139.9
								3000	204.2	340.3
E322	0.375	0.250	0.46	0.119	0.125	1.47	1.67	1000	183.2	305.3
								3000	500.3	833.8

Table T2.3a Configuration 3: Stability of bed protection;
 Near-bed structure: $D_{n50} = 7.2$ mm, slope 1:3;
 Bed protection: $D_{n50} = 3.1$ mm.

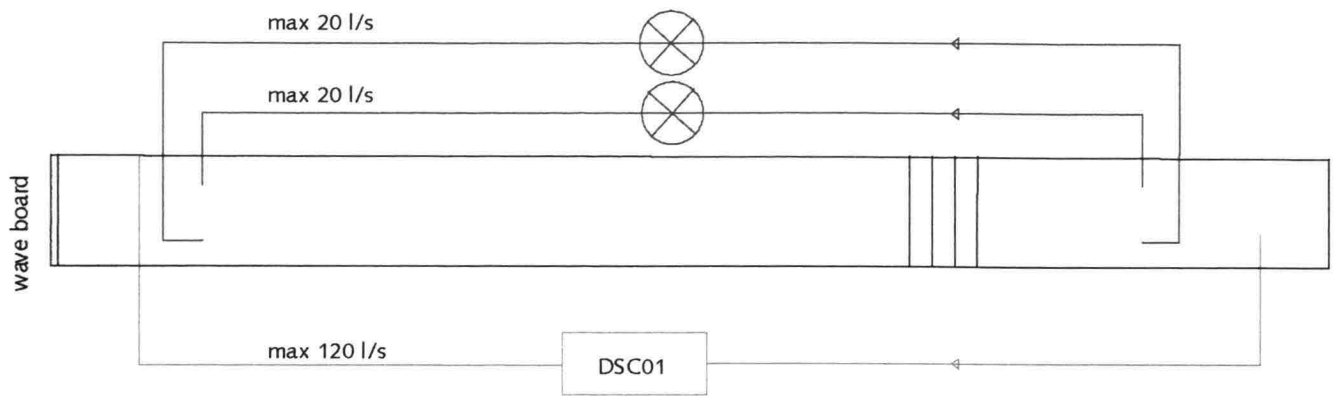
Stability of near-bed structure										
No.	Water depth		Velocity	Waves					Damage	
	h	h_{crest}	u_c	$H_{1/3}$	H_{m0}	T_m	$T_{m-1,0}$	N_{waves}	N_{od}	S
A310	0.500	0.375	0	0.090	0.094	1.11	1.17	1000	2.6	4.4
								3000	3.7	6.1
A311	0.500	0.375	0	0.127	0.133	1.32	1.42	1000	2.8	4.6
								3000	4.4	7.3
A312	0.500	0.375	0	0.163	0.170	1.51	1.67	1000	3.8	6.3
								3000	4.4	7.4
H312 =A312	0.500	0.375	0	0.162	0.169	1.51	1.67	1000	3.8	6.3
								3000	7.8	13.0
A313	0.500	0.375	0	0.188	0.197	1.66	1.86	1000	5.0	8.3
								3000	7.1	11.8
H313 =A313	0.500	0.375	0	0.186	0.197	1.66	1.86	1000	3.5	5.9
								3000	6.0	10.0
A320	0.375	0.250	0	0.085	0.090	1.10	1.17	1000	2.6	4.3
A321	0.375	0.250	0	0.119	0.126	1.32	1.45	1000	1.3	2.1
								3000	3.5	5.8
A322	0.375	0.250	0	0.144	0.152	1.51	1.70	1000	5.3	8.9
								3000	10.4	17.4
B320	0.375	0.250	0.11	0.078	0.084	1.08	1.16	1000	1.7	2.9
B321	0.375	0.250	0.10	0.112	0.118	1.29	1.45	1000	1.8	3.0
								3000	3.8	6.3
B322	0.375	0.250	0.10	0.135	0.143	1.47	1.69	1000	2.0	3.3
								3000	6.0	10.0
D320	0.375	0.250	0.35	0.067	0.072	1.12	1.20	1000	8.8	14.6
D321	0.375	0.250	0.35	0.098	0.104	1.30	1.45	1000	1.2	2.0
								3000	1.9	3.1
D322	0.375	0.250	0.35	0.122	0.129	1.46	1.67	1000	0.6	1.0
								3000	0.8	1.3
V322	0.375	0.250	0.35	0	0	0	0	0	4.4	7.4
V323	0.375	0.250	0.46	0	0	0	0	0	17.0	28.3

Table T2.3b Configuration 3: Stability of near-bed structure;
 Near-bed structure: $D_{n50} = 7.2$ mm, slope 1:3;
 Bed protection: $D_{n50} = 3.1$ mm.

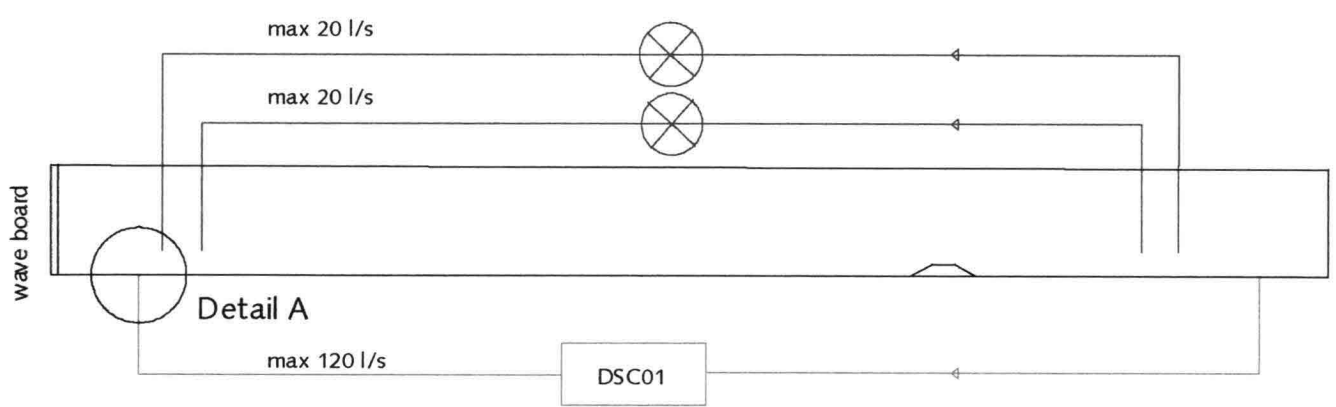
Stability of near-bed structure										
No.	Water depth		Velocity	Waves					Damage	
	h	h_{crest}	u_c	$H_{1/3}$	H_{m0}	T_m	$T_{m-1.0}$	N_{waves}	N_{od}	S
A410	0.500	0.375	0	0.090	0.094	1.11	1.17	1000	13.4	22.3
								3000	22.4	37.3
A411	0.500	0.375	0	0.127	0.134	1.32	1.42	1000	11.1	18.5
								3000	25.8	43.0
A412	0.500	0.375	0	0.164	0.171	1.51	1.67	1000	62.1	103.6
								3000	123.8	206.4
A413	0.500	0.375	0	0.190	0.199	1.66	1.86	1000	187.0	311.7
								3000	432.1	720.2
C410	0.500	0.375	0.20	0.076	0.080	1.09	1.18	1000	10.8	18.0
								3000	15.0	25.0
C411	0.500	0.375	0.19	0.113	0.119	1.28	1.43	1000	8.4	14.1
C412	0.500	0.375	0.18	0.147	0.153	1.49	1.66	1000	6.2	10.4
								3000	11.4	18.9
C413	0.500	0.375	0.18	0.172	0.181	1.62	1.83	1000	17.4	28.9
								3000	26.5	44.2
D413	0.500	0.375	0.32	0.163	0.171	1.60	1.82	1000	13.2	22.0
								3000	28.4	47.3
F423	0.375	0.250	0.74	0.141	0.149	1.57	1.80	1000	461.4	769.0
								3000	818.0	1363.4
V411	0.500	0.375	0.20	0	0	0	0	0	8.4	14.1
V412	0.500	0.375	0.34	0	0	0	0	0	9.2	15.4
V413	0.500	0.375	0.46	0	0	0	0	0	13.7	22.9

Table T2.4 Configuration 4: Stability of near-bed structure;
 Near-bed structure: $D_{n50} = 3.1$ mm, slope 1:8;
 Bed protection: $D_{n50} = 3.1$ mm.

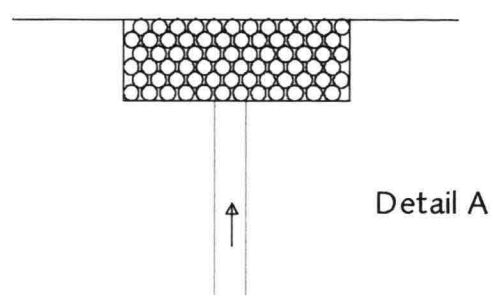
Figures



Plan View



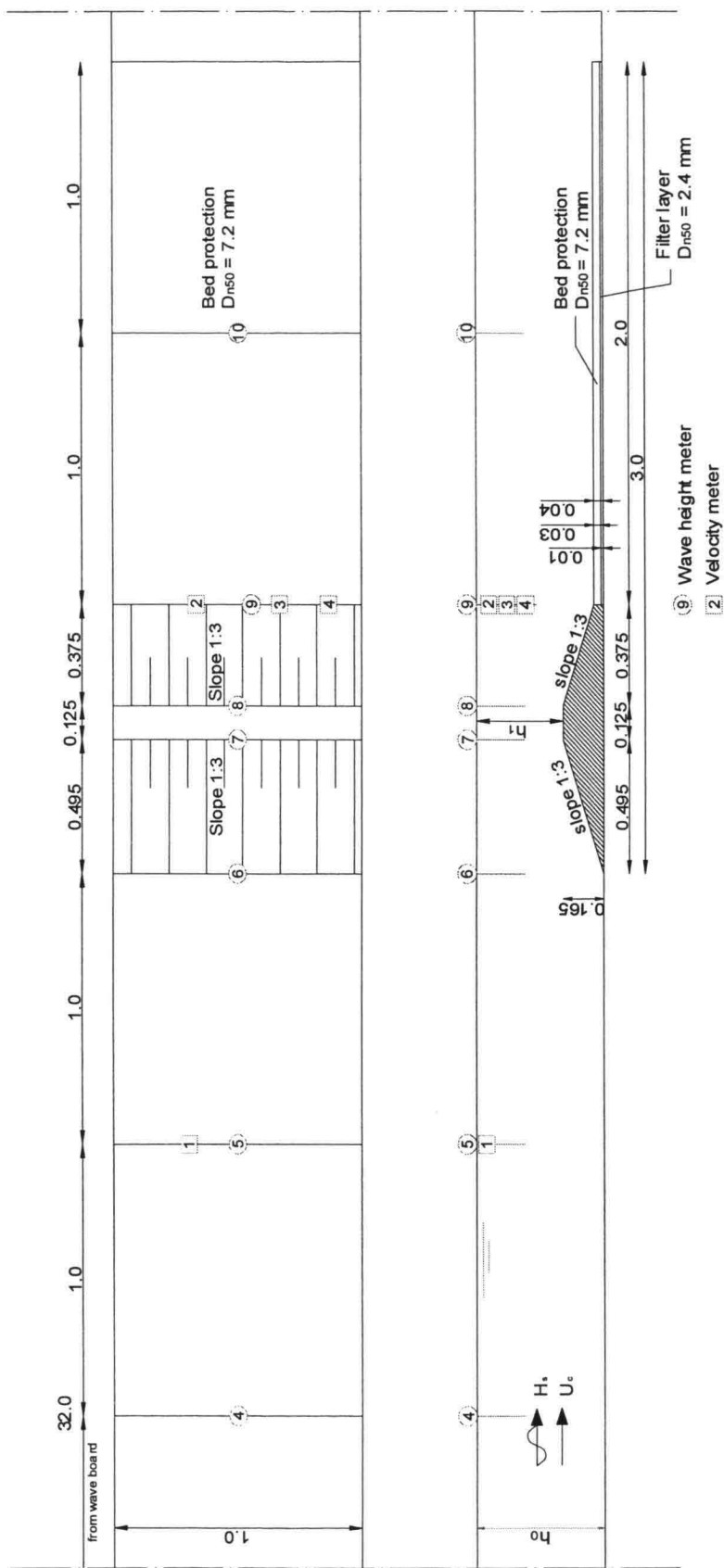
Side View



Detail A

Circuit of currents in the Scheldt flume

Not to scale



Cross section and plan view

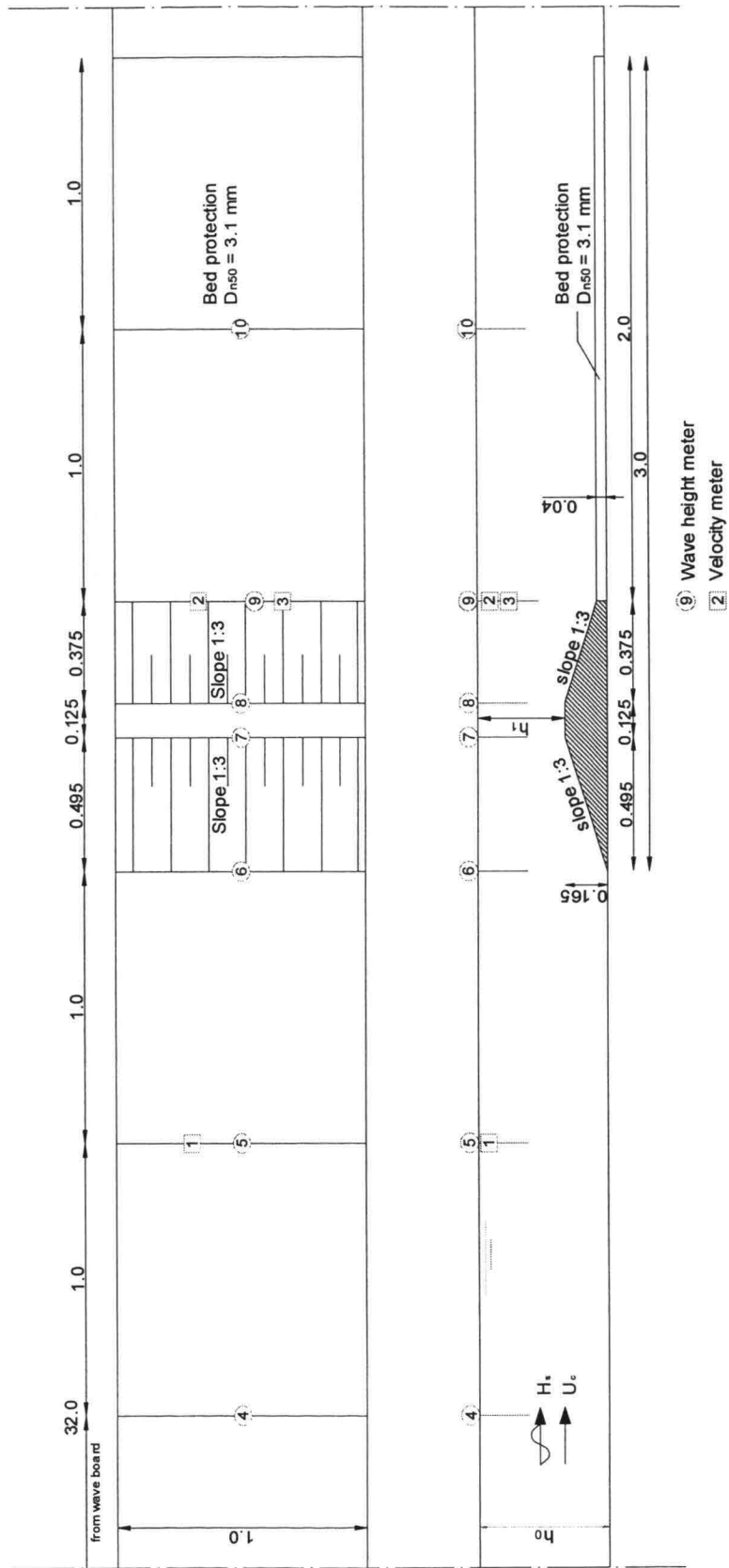
for Configuration 1

Not to scale

WL | DELFT HYDRAULICS

H3804

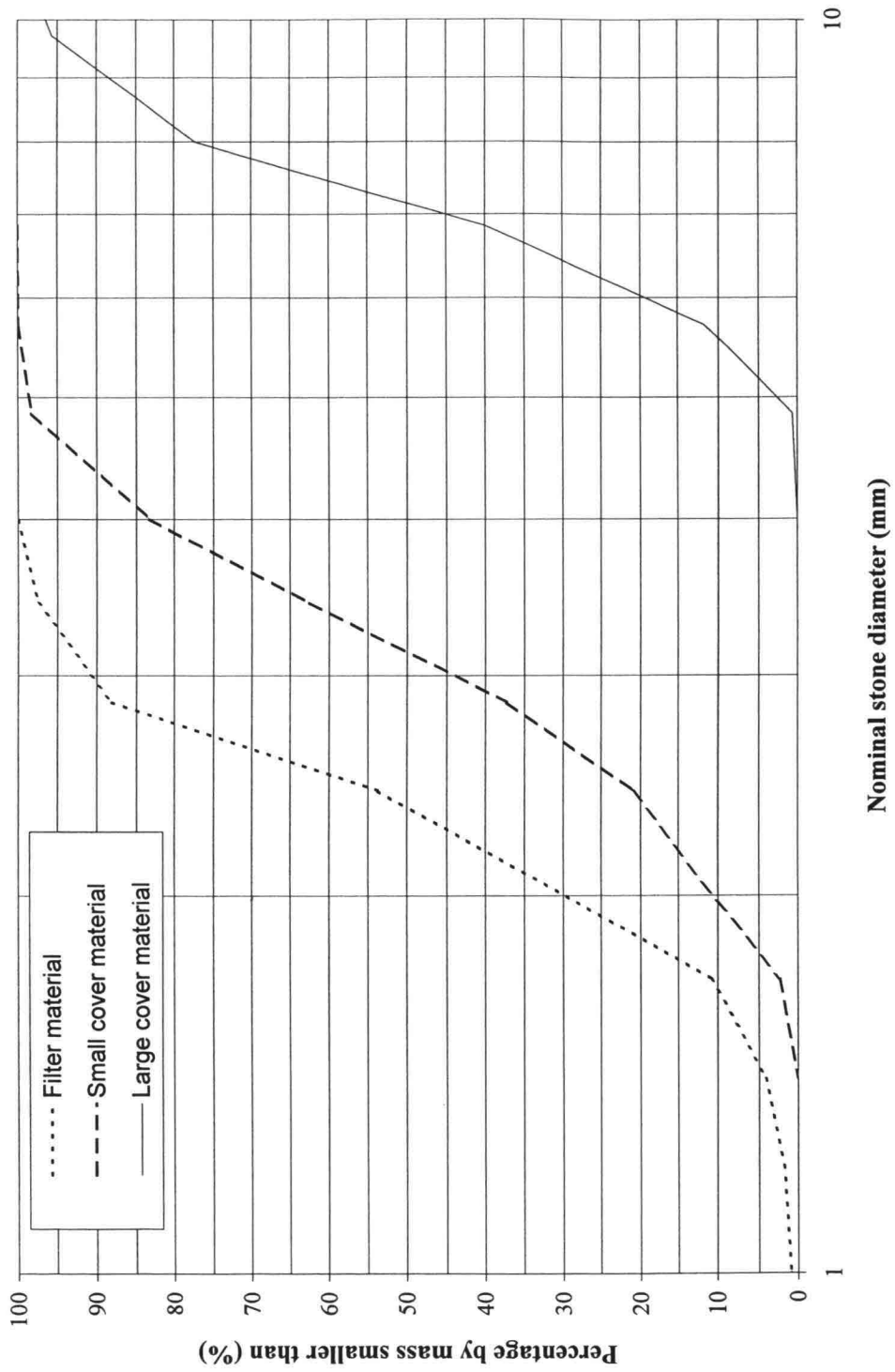
Fig. F2.2



Cross section and plan view
for Configuration 2

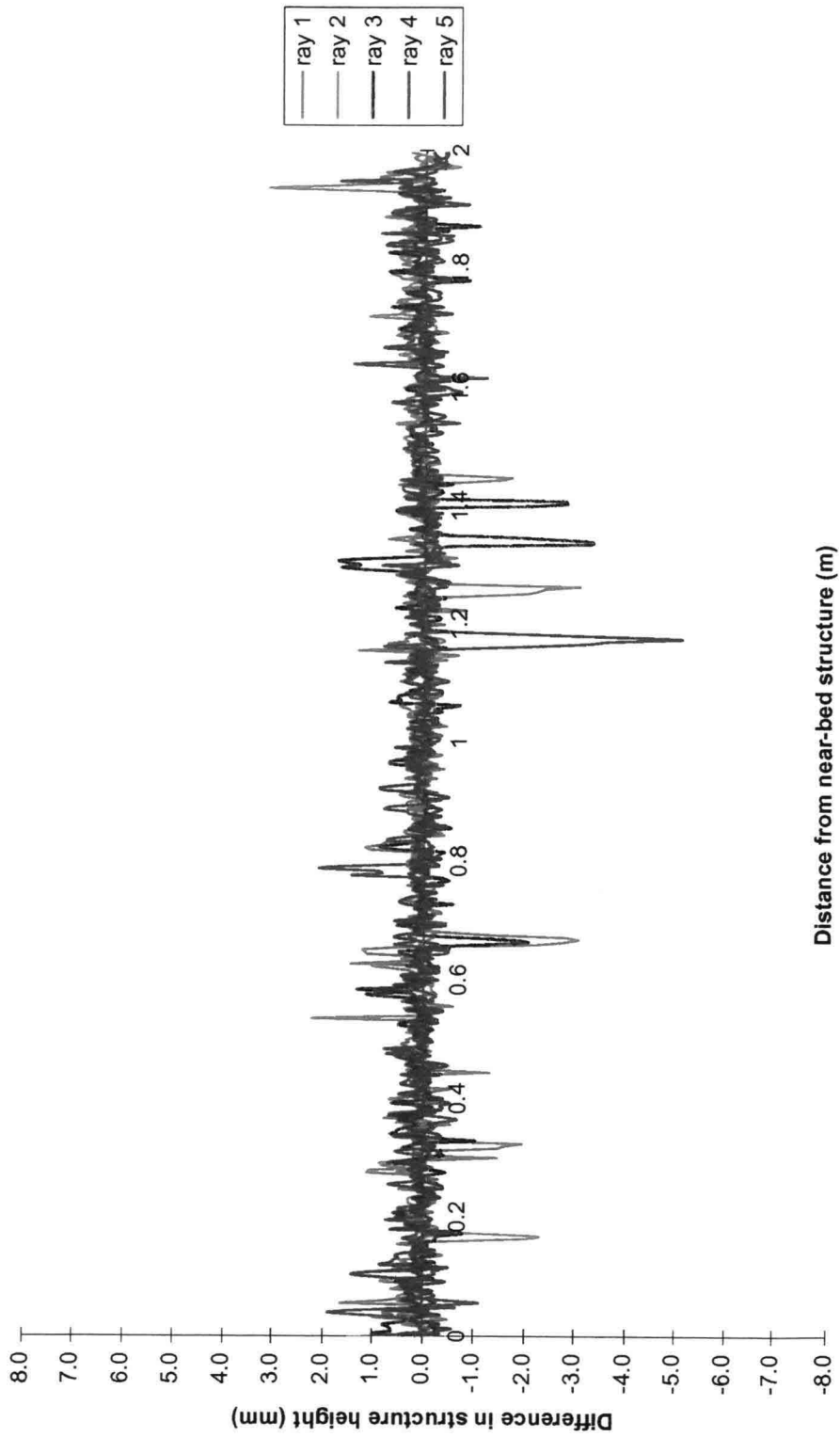
Not to scale

Rock armour gradations



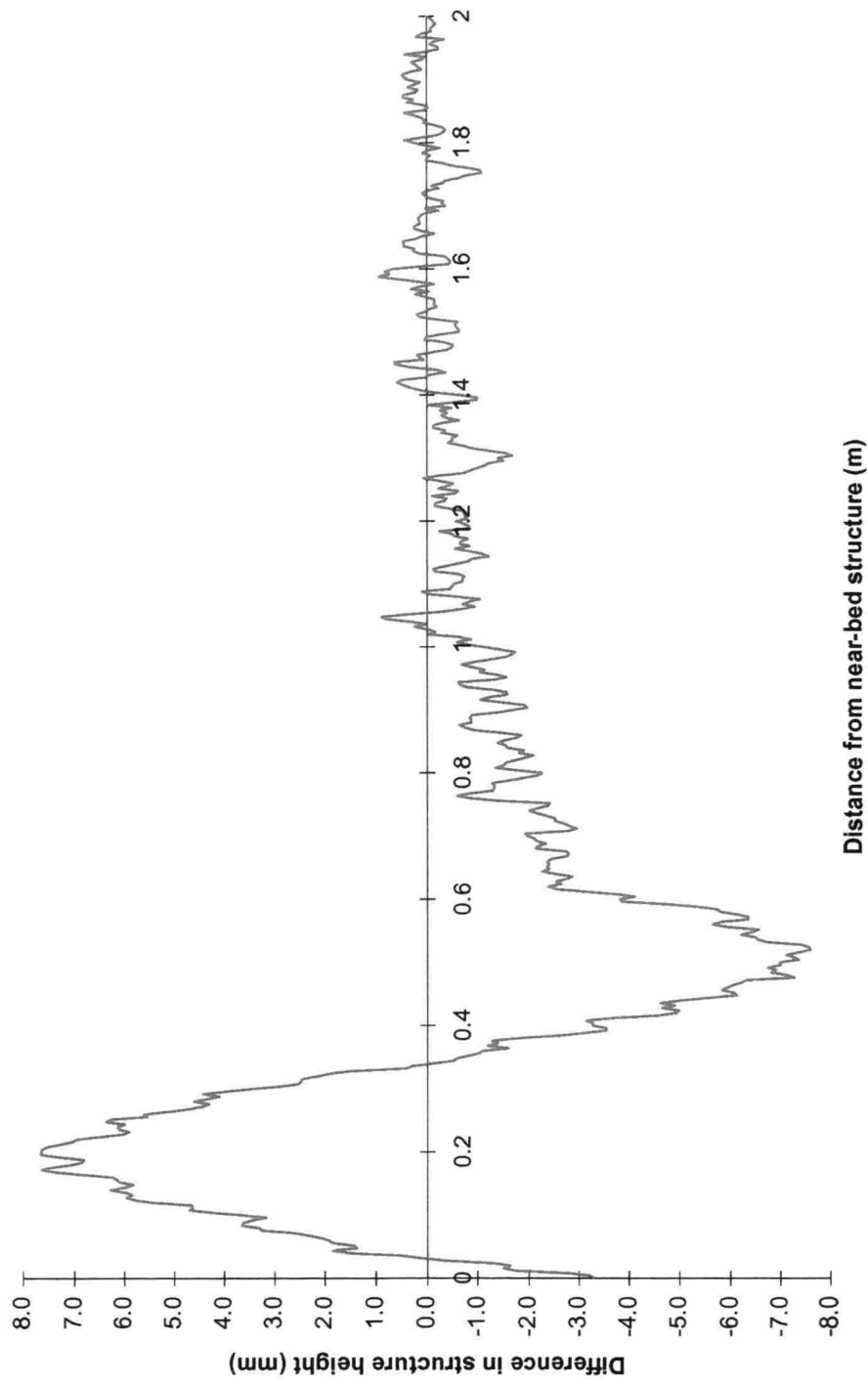
Grading curves

Filter and cover layers



Example of measured erosion profile
(low amount of erosion)

Test C122



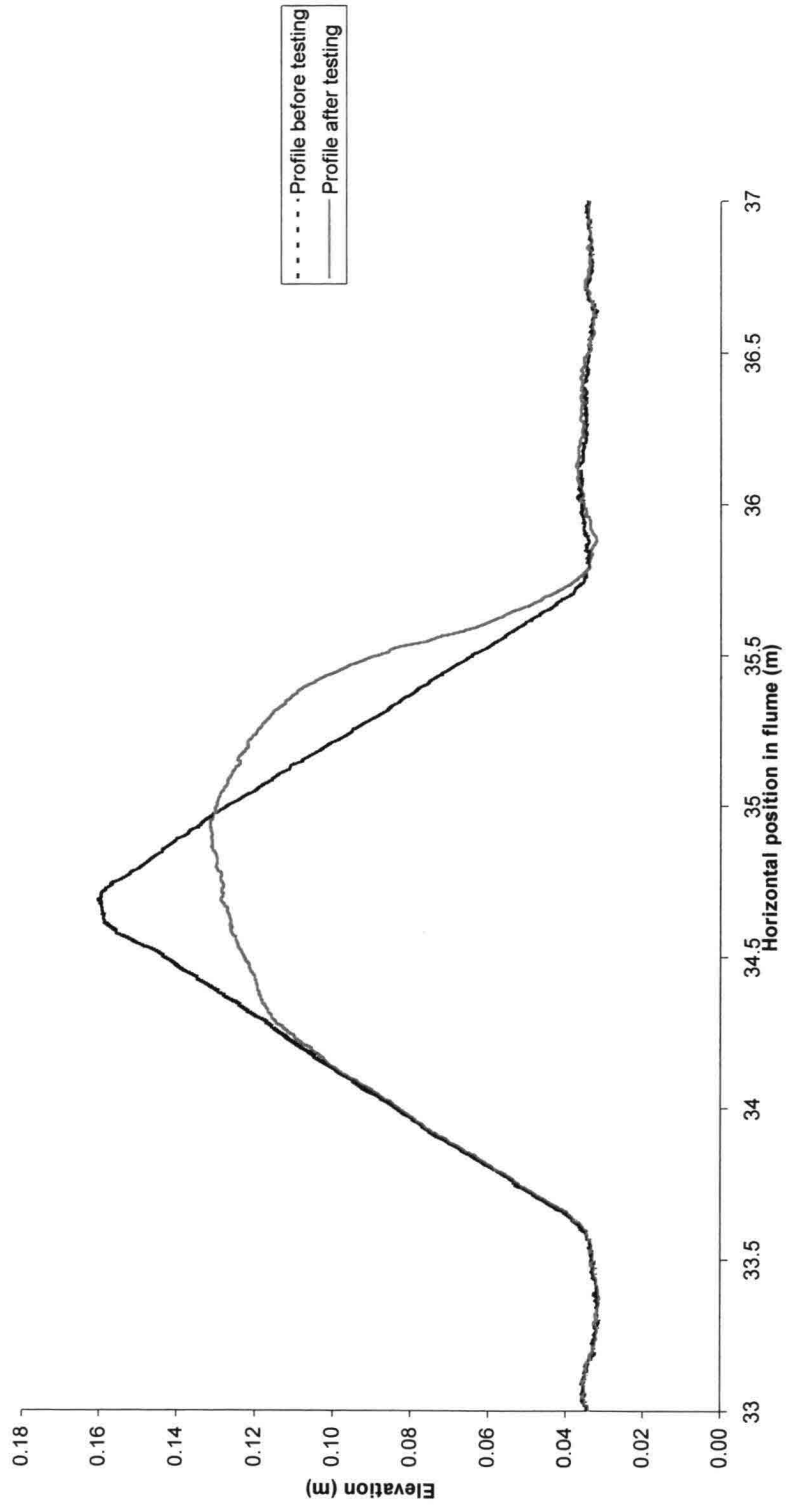
Example of measured erosion profile
(high amount of erosion)

Test E221

WL | DELFT HYDRAULICS

H3804

Fig. F2.8



Measured profile after test F423
(near-bed structure)

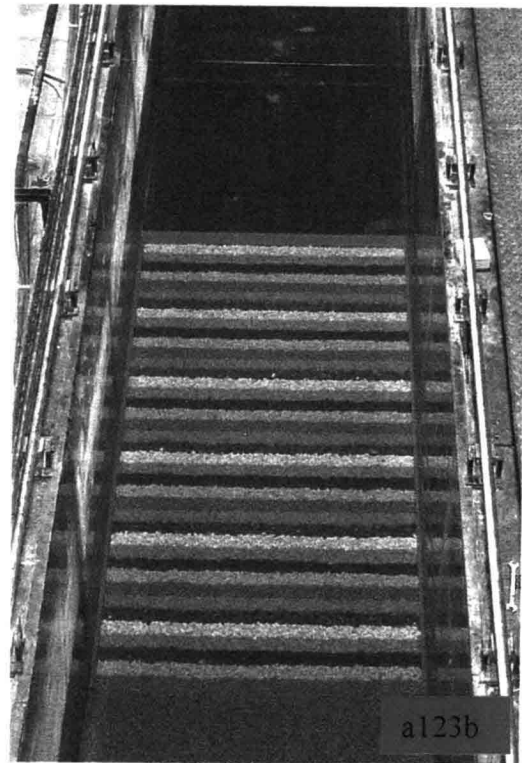
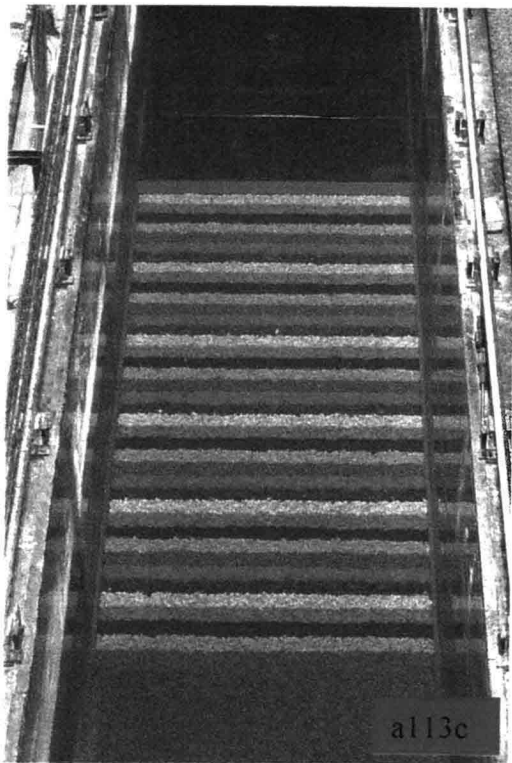
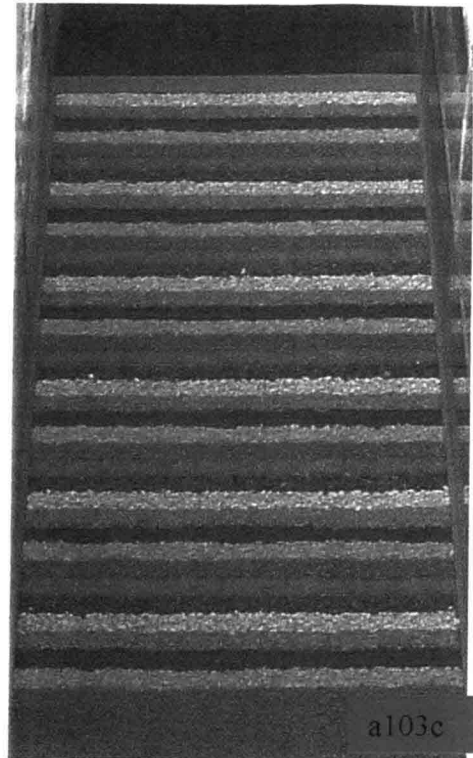
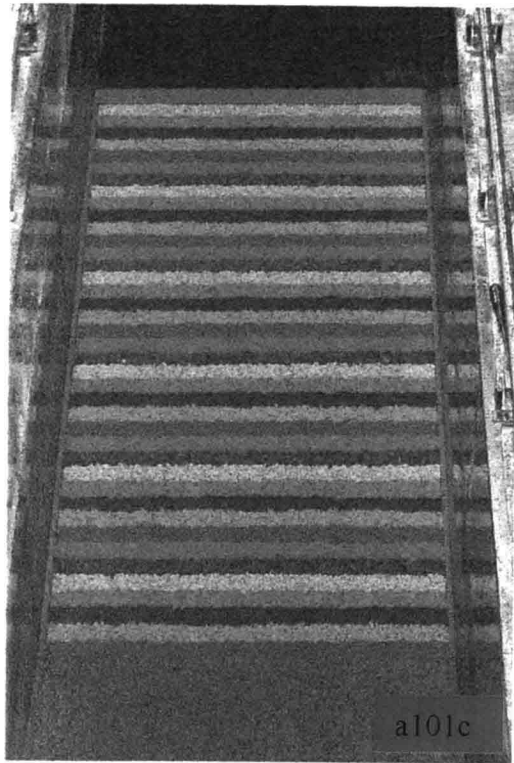
Test F423

WL | DELFT HYDRAULICS

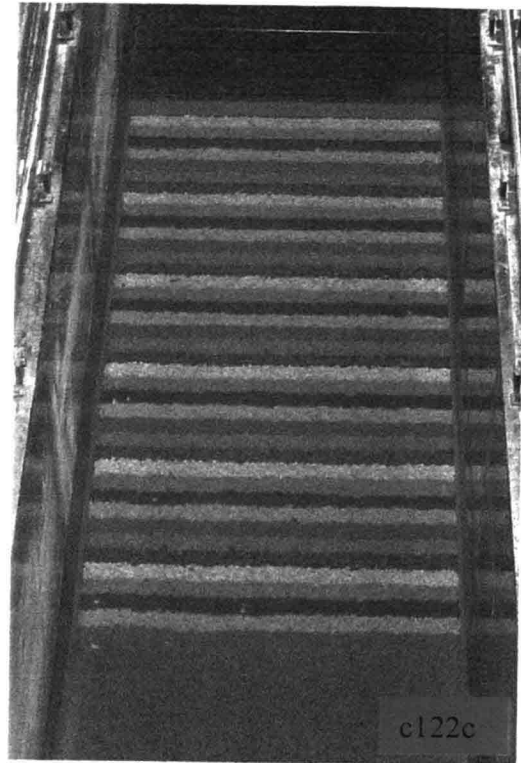
H3804

Fig. F2.9

Photographs



Photographs Configuration 1



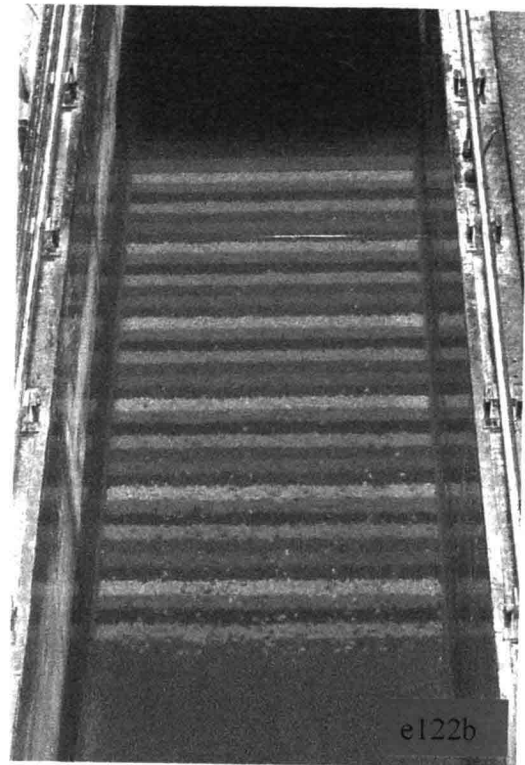
Photographs Configuration 1



Photographs Configuration 1



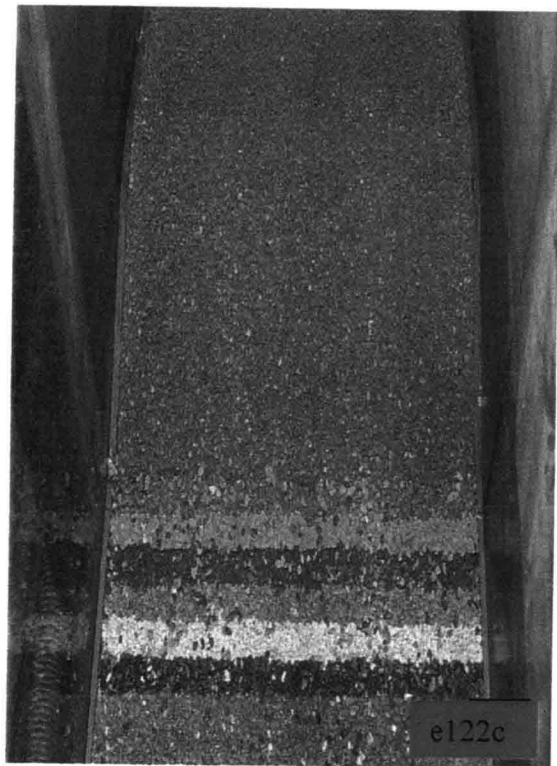
e122a



e122b

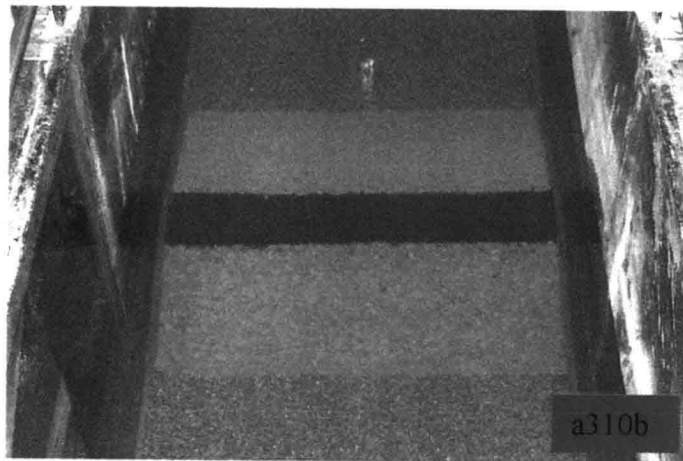


e122c

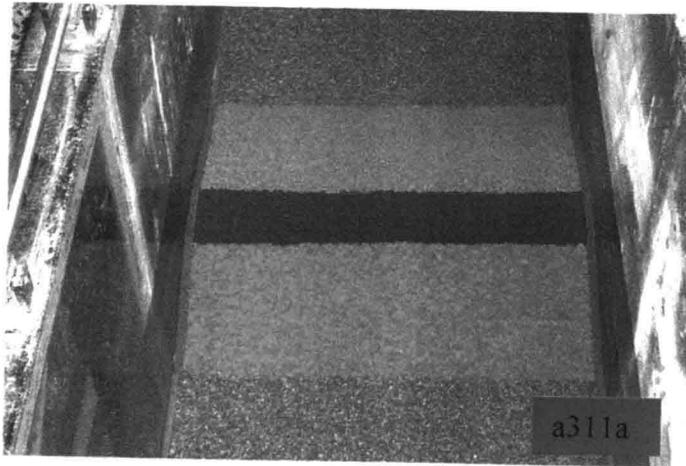


e122c

Photographs Configuration 1



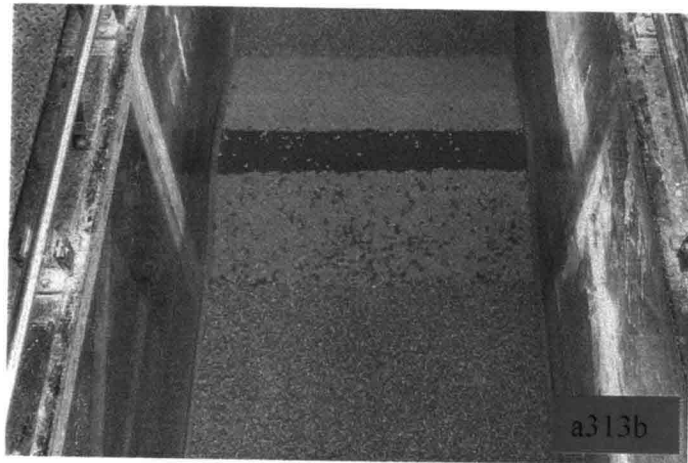
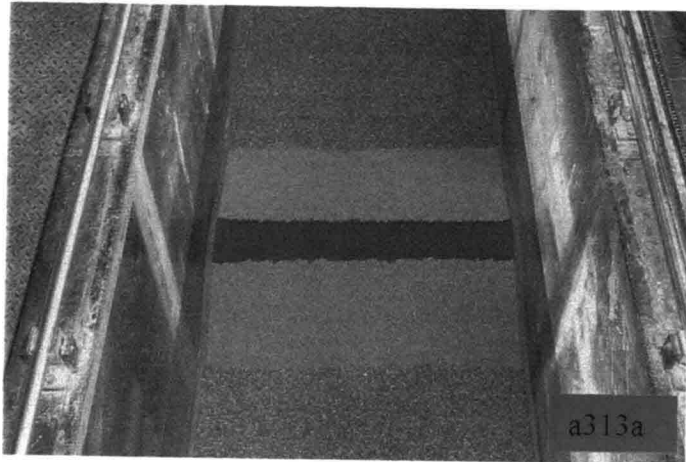
Photographs Configuration 3



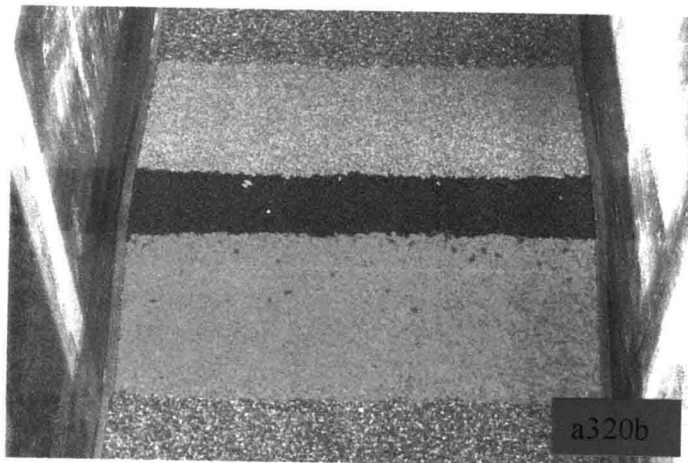
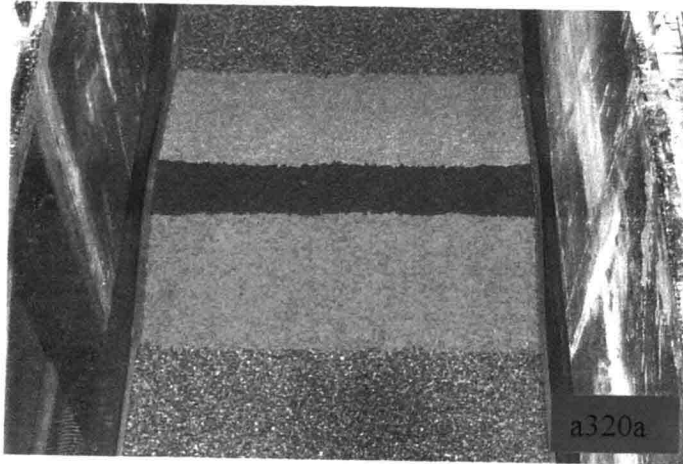
Photographs Configuration 3



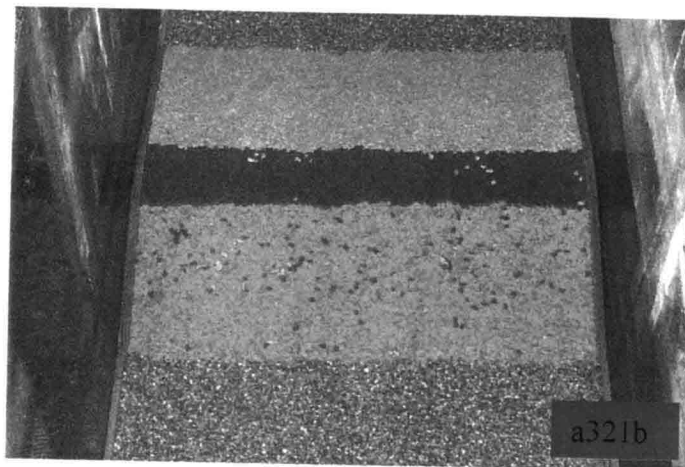
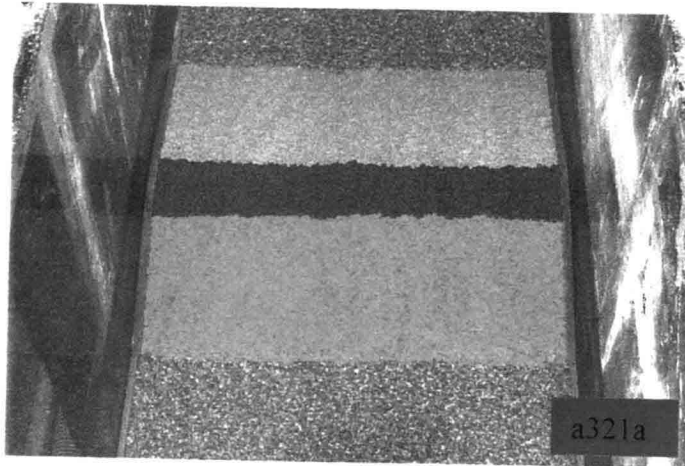
Photographs Configuration 3



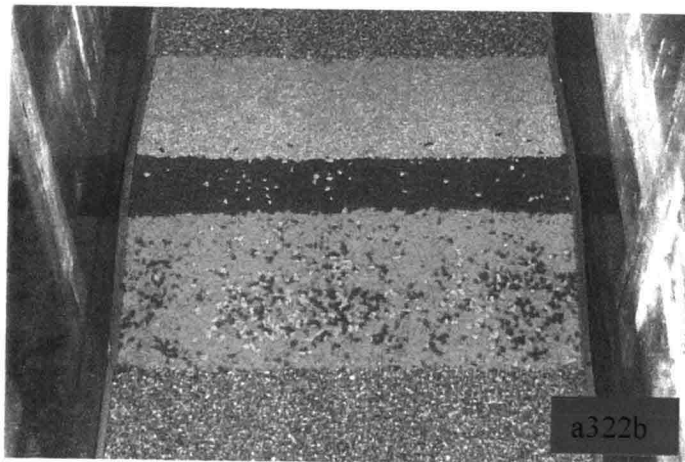
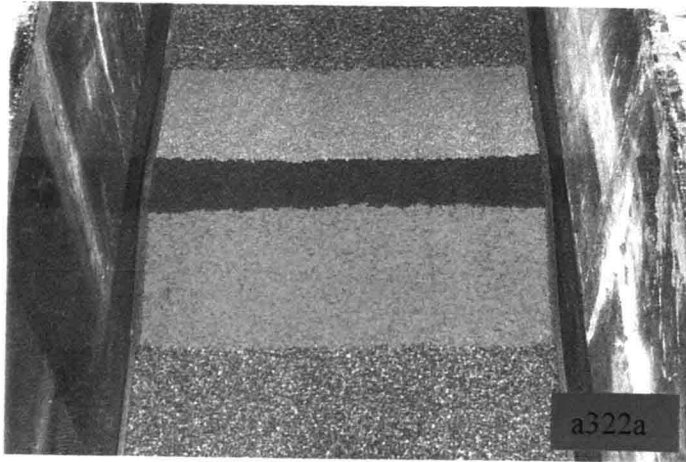
Photographs Configuration 3



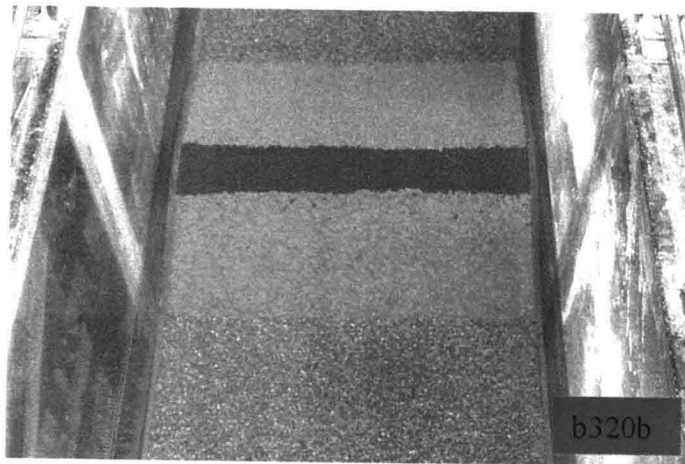
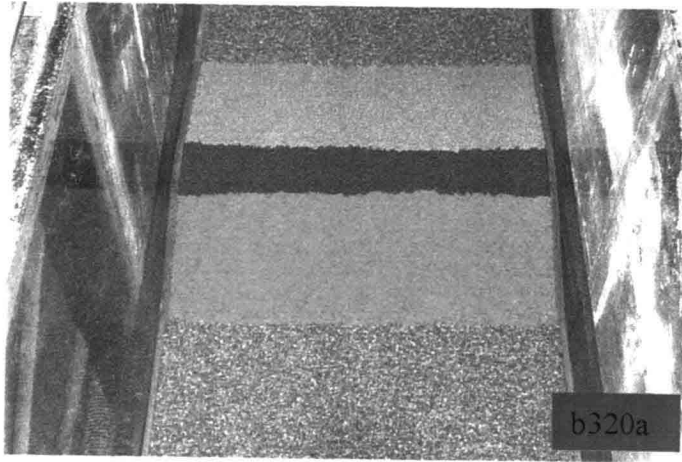
Photographs Configuration 3



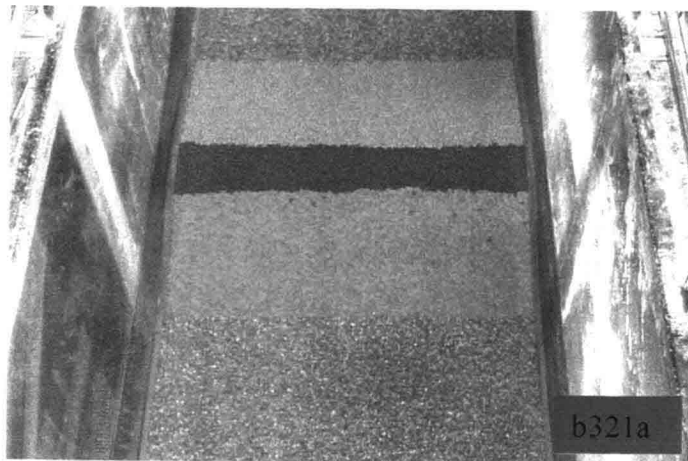
Photographs Configuration 3



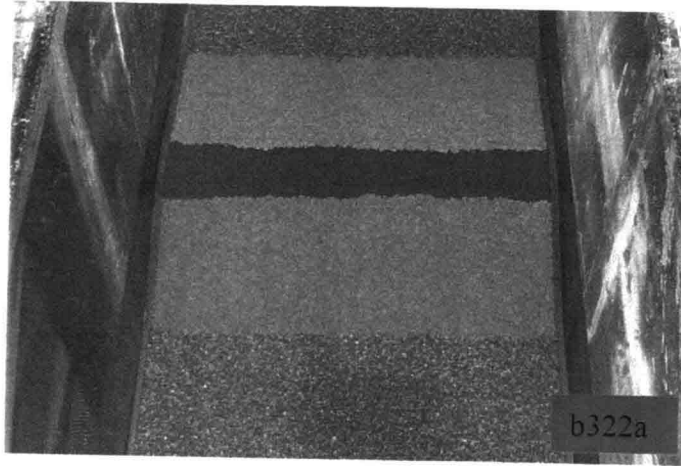
Photographs Configuration 3



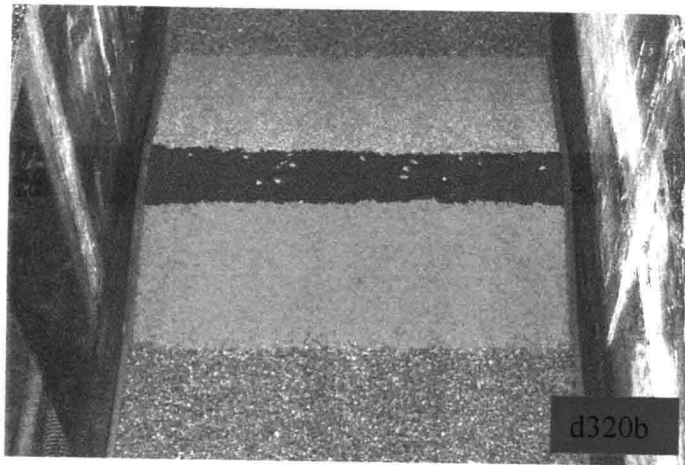
Photographs Configuration 3



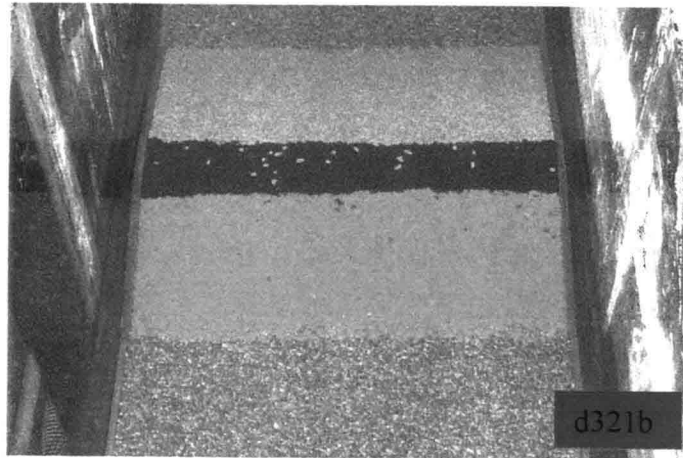
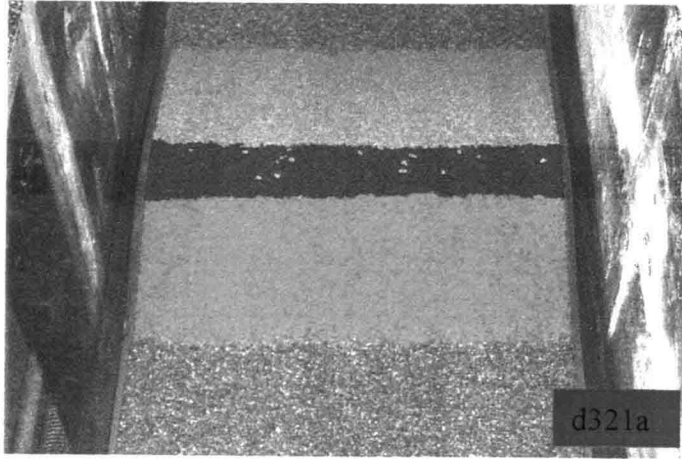
Photographs Configuration 3



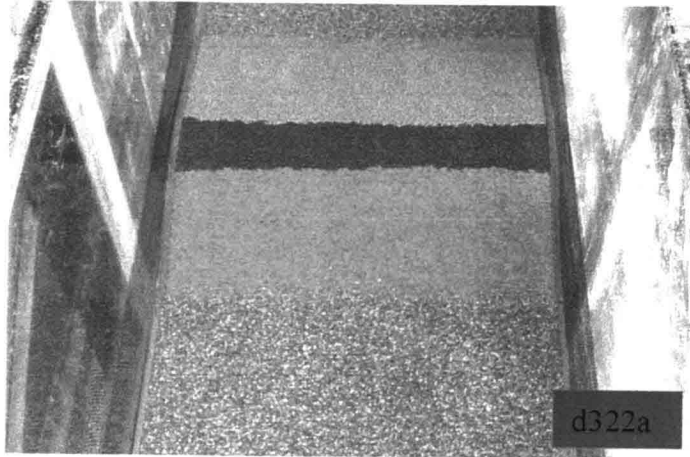
Photographs Configuration 3



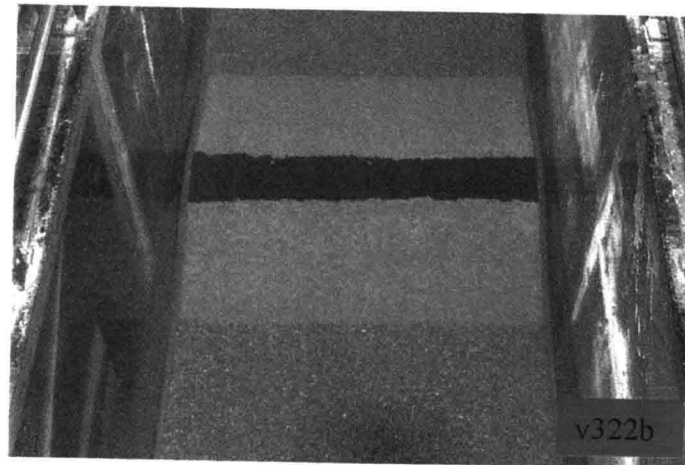
Photographs Configuration 3



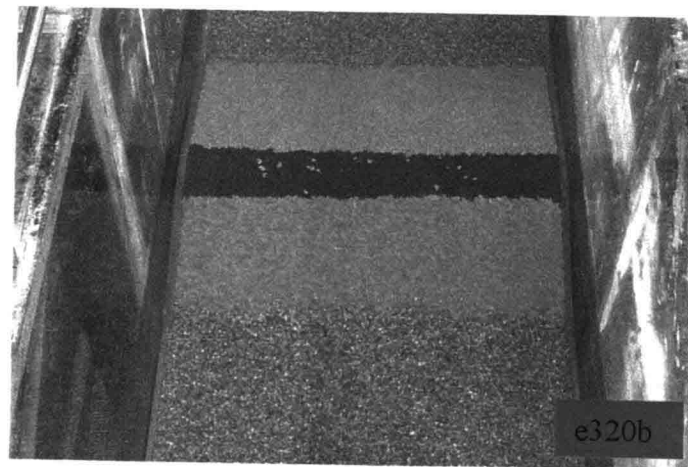
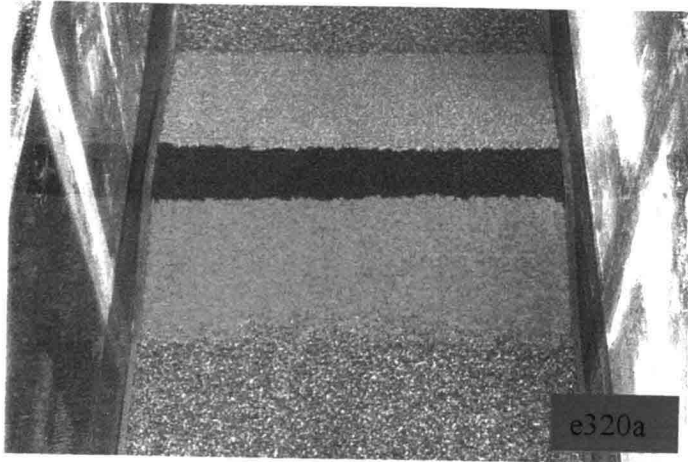
Photographs Configuration 3



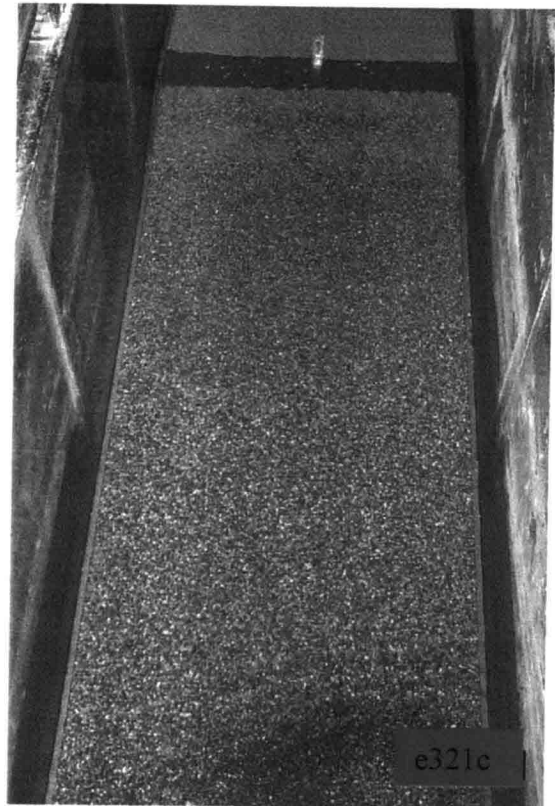
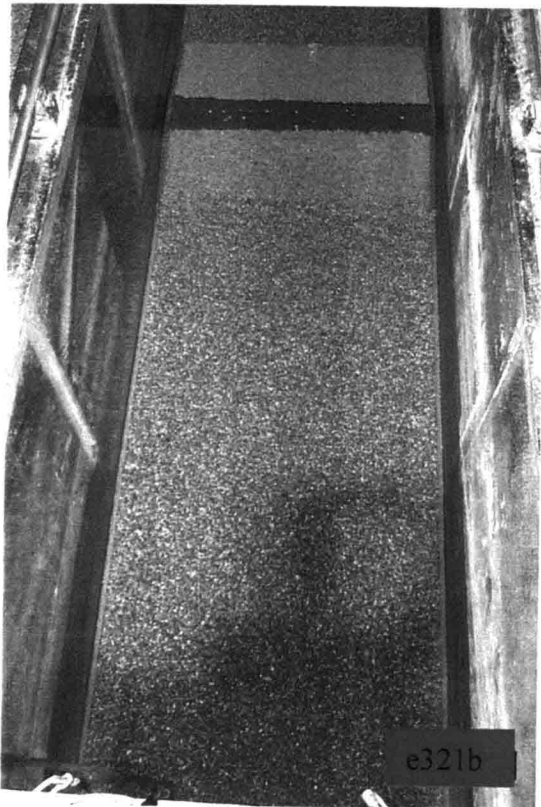
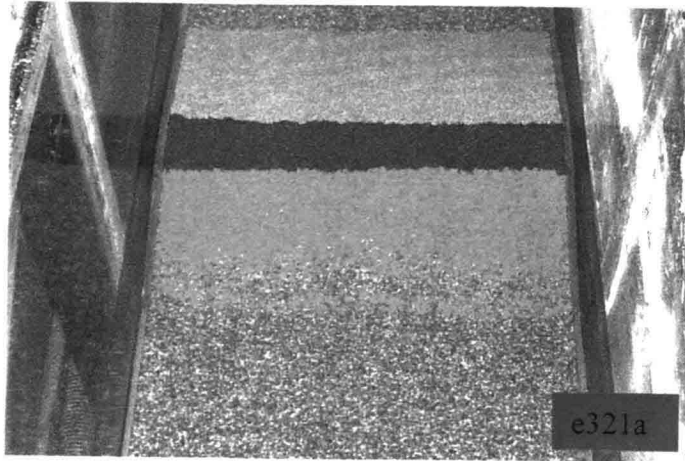
Photographs Configuration 3



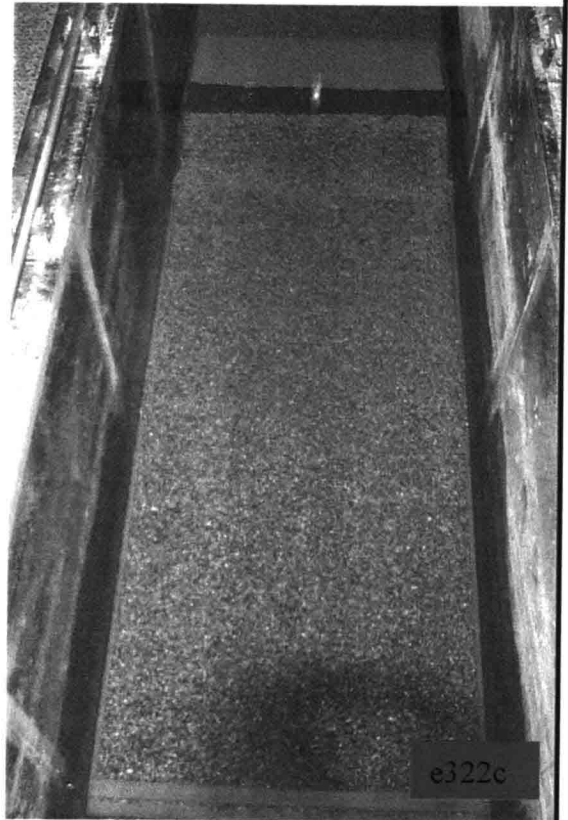
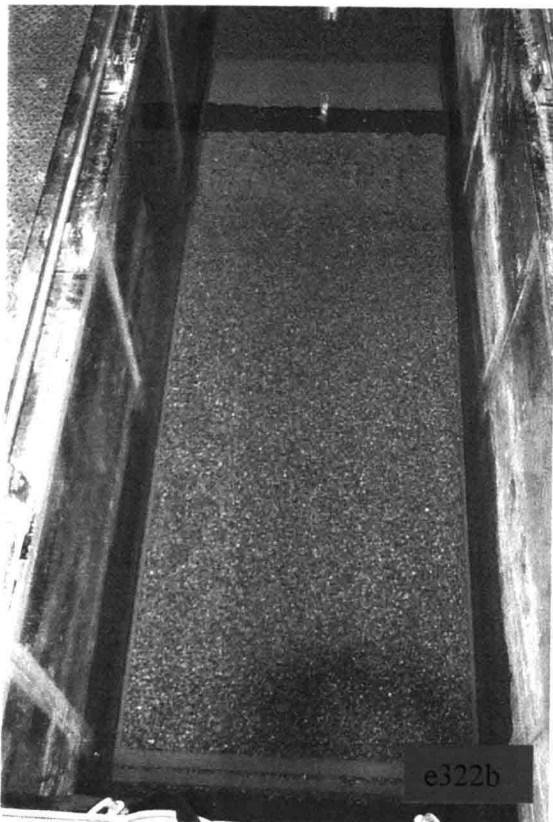
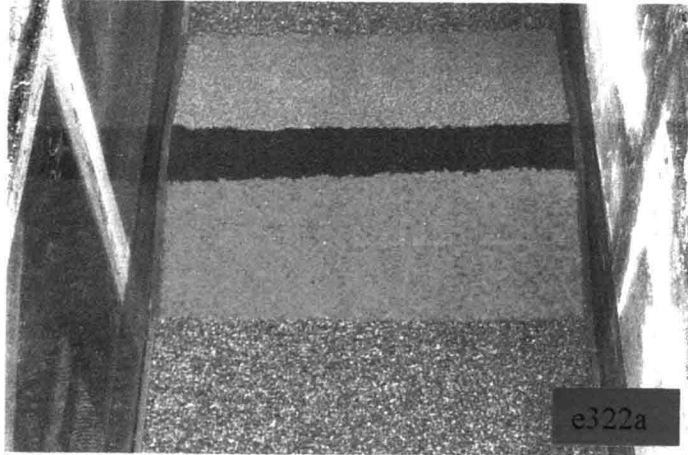
Photographs Configuration 3



Photographs Configuration 3



Photographs Configuration 3



Photographs Configuration 3



